Lawrence Berkeley National Laboratory
Recent Work

Title
Bevalac Extraction

Permalink

Authors
Kalnins, J.G.
Krebs, G.
Tekawa, M.
et al.

Publication Date
1992-02-01

Lawrence Berkeley Laboratory
UNIVERSITY OF CALIFORNIA
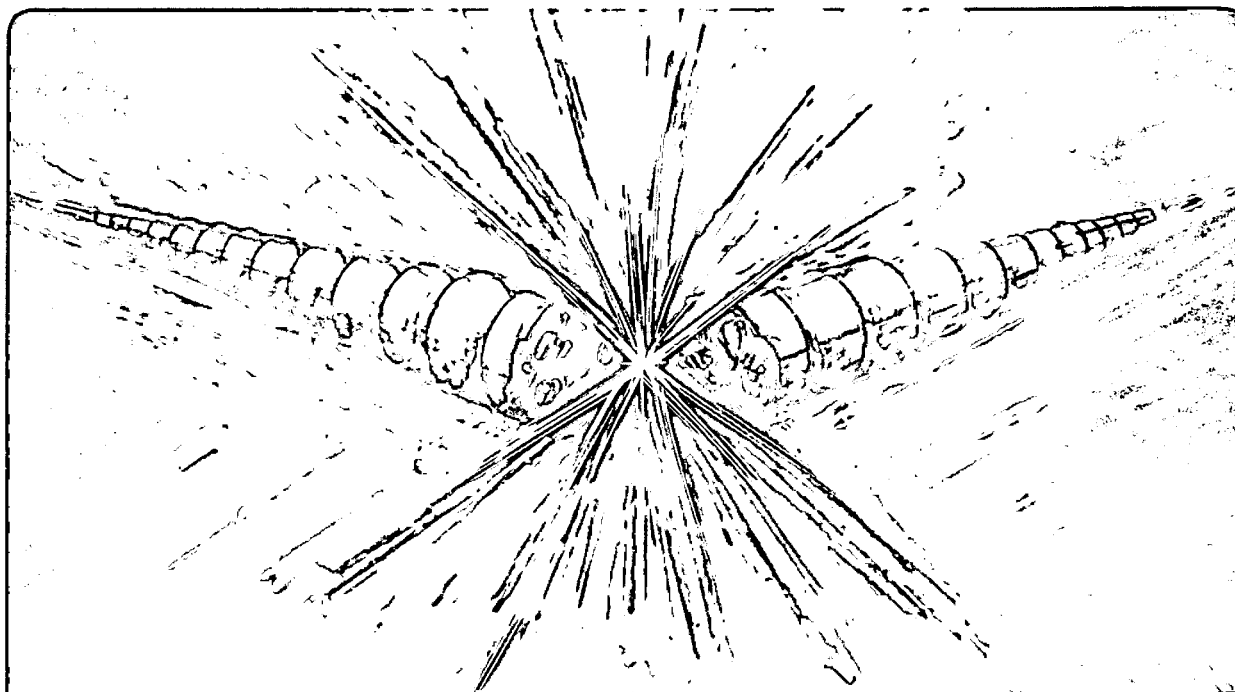
Accelerator & Fusion Research Division

Bevalac Extraction

J.G. Kalnins, G. Krebs, M. Tekawa, D. Cowles, and T. Byrne

February 1992

DISCLAIMER

DISCLAIMER

Bevalac Extraction

J. G. Kalnins, G. Krebs, M. Tekawa, D. Cowles, T. Byrne

ACCELERATOR FUSION RESEARCH DIVISION
Lawrence Berkeley Laboratory
University of California
Berkeley, California 94720

November, 1991

Bevalac Extraction.

J.G.Kalnins, G.Krebs, M.Tekawa,
D.Cowles, T.Byrne.
November 11, 1991.

This report will describe some of the general features of the Bevatron extraction system, primarily the dependence of the beam parameters and extraction magnet currents on the Bevalac field. The extraction magnets considered are: PFW (Pole-Face-Windings) , XP1, XP2 , XS1, XS2 , XM1, XM2 , XM3 , XQ3A and XQ3B. A schematic of their location is shown in Fig.1 and Fig.2. This study is based on 84 past tunes (from 1987 to the present) of various ions (p,He,O,Ne,Si,S,Ar,Ca,Ti,Fe,Nb,La,Au and U), for Bevalac fields from 1.749 to 12.575 kG, where all tunes included a complete set of beam line wire chamber pictures.

The circulating beam intensity inside the Bevalac is measured with Beam Induction Electrodes (BIE) in the South Tangent Tank. The extracted beam intensity is usually measured with the Secondary Emission Monitor (SEM) in the F1-Box. For most of the tunes the extraction efficiency, as given by the SEM/BIE ratio, was not recorded in the MCR Log Book, but plotting the available Log Book data as a function of the Bevalac field, see Fig.9, we find that the extraction efficiency is typically between 30->60% with feedback spill.

(1) <u>The Bevalac extraction field</u> (B_{ev}).

Knowing the Bevalac field during extraction (B_{ev}) allows one to calculate the rigidity (R_B) of the beam exiting the machine:

$$R_B = B_{ev} \, r_B \qquad\qquad (1)$$

where B_{ev} = Bevalac field (12.575 kG maximum)

r_B = beam radius

The beam is normally extracted at a nominal radius of 600" (see Sec.(4)), so the maximum beam rigidity out of the Bevalac is nominally 192 kG-m.

If the extraction magnets do not saturate, and the beam directions for dipoles, or focal points for quadrupoles, at extraction

are the same for all Bevalac fields, then all the dipole and quadrupole magnet currents $,I_M,$ for the external transport lines, should scale linearly with the beam rigidity R_B, or the Bevalac field B_{ev} (Eqn.(1)).

(2) Extracted Beam Emittance.

In a drift space, the beam size x as a function of the downstream position L, is given from linear optics by the quadratic envelope equation:

$$x^2 = x_0{}^2 + x'_0{}^2 (L - L_{xo})^2 \qquad (2a)$$

with limit: $\qquad x \approx x'_0 (L - L_{xo}) \qquad$ for $\quad L \to \infty \qquad (2b)$

$$\text{or} \quad (L - L_{xo}) >> \beta_{xo}$$

By measuring the beam size (FWHM) in the EPB0 drift space at the exit of the machine at three locations (wire chambers XQ3WC, XF1WC and XM4WC), we can calculate the following horizontal (x) and vertical (y) beam parameters:

(a) The location $,L_{xo},$ of the F1-focus (waist): The Bevalac operators normally tune the XQ3 quadrupoles to produce a horizontal and vertical waist at XF1WC (which is chosen as the origin: $L = 0$).

(b) The beam size $,x_0,$ at the waist: This is the beam size as measured at XF1WC, if the operators have tuned the XQ3 quadrupoles properly to focus the beam there.

(c) The beam divergence $,x'_0,$ at the waist: We can estimate the beam divergence at F1 from the beam size $,x_{M4},$ at XM4WC, using Eqn.(2b): $\qquad x'_0 \approx 0.16 \, x_{M4} \quad$ (mr/mm)

If the beam size magnification at some downstream focal-point F is measured as $x_F/x_0 = m_{xF}$, then the beam divergence will scale as $x'_F/x'_0 = 1/m_{xF}$.

(d) The F1 beta-function $,\beta_{xo},$ can be calculated from the beam size and divergence: $\qquad \beta_{xo} = x_0/x'_0 \qquad\qquad (3)$

The beta-function determines the optics in the external particle beam lines. That is, two beams with the same initial β_{xo} at F1, will have beam sizes at any point downstream, that scale with

2

the emittance as: $x_2/x_1 = \sqrt{(E_{x2}/E_{x1})}$

(e) The beam emittance , E_x, can also be calculated from the beam size and divergence: $E_x = \pi\, x_o\, x'_o$ (4)

and the normalized emittance is then: $E_{nx} = E_x\, \gamma\beta$

here $\gamma\beta$ can be calculated from the beam momentum

$$pc = AW_o\, \gamma\beta \qquad (5)$$

where   A = ion mass (Amu)

                  $W_o = 931.5016$ MeV/A

and $\gamma = 1/\sqrt{(1-\beta^2)}$

                $\beta = v/c$ = beam velocity/velocity of light

or can be calculated from the beam rigidity

$$R_B = R_o\, \gamma\beta/(Q+/A)$$

where   (Q+/A) = charge/mass

             $R_o = 31.07155$ kG-m

In any transport line the transverse emittances E_x and E_y of a beam (monoenergetic, $\Delta p/p = 0$, or dispersionless, $\eta_x = 0$) will be constant (Liouville's Theorem).

The beam in the Bevatron during acceleration undergoes adiabatic betatron-damping. Ideally this will reduce the emittance with increasing beam momentum, but will keep the normalized-emittances E_{nx} and E_{ny} constant.

For most of the tunes studied, we only know the beam size at wire chambers XF1WC and XM4WC. For these cases, we used the approximation that the F1-focus was at XF1WC, to calculate the beam parameters.

The beam size, beam divergence and the beta-function at F1 as a function of the Bevalac field, is shown for the horizontal plane in Fig.11 and the vertical plane in Fig.12. We observe that while the horizontal and vertical beam size decreases with increasing Bevalac field, the beam divergence remains about the same (2->4 mr).

If we look at the extracted beam emittance, Fig.13(a) and (b), it shows that both the horizontal and vertical emittances decrease with increasing Bevalac field (increasing momentum). However, this is not totally due to betatron-damping, since the normalized emittances increase with momentum (Fig.14(a) and (b)).

The average horizontal and vertical beam emittances at the SuperHilac exit have been measured[2] as

3

$$E_x = 10.2 \pm 2.3 \; \pi \text{ mm-mr}$$

$$E_y = 11.2 \pm 3.8 \; \pi \text{ mm-mr}$$

with normalized emittances (Tank 8: Beam energy 8.5 MeV/A)

$$E_{nx} = 1.4 \pm 0.3 \; \pi \text{ mm-mr}$$

$$E_{ny} = 1.5 \pm 0.5 \; \pi \text{ mm-mr}$$

Comparing the normalized emittances the beam has before injection, with that measured after extraction, see Fig.14(a) and (b), we observe an order of magnitude emittance growth. Horizontally, we expect an emittance growth from the multi-turn injection and the nonlinear resonant extraction. Vertically, the growth indicates that extraction takes place near a vertical resonance.

(3) Tailwag/Feedback spill (see also Sec.6).

The RF is normally turned off during flattop to eliminate a RF fine structure on the extracted beam. The two standard ways of spilling the beam are:

(a) Tailwag spill.

A tailwag spill is usually used for low Bevalac fields to give better extraction efficiency. The typical tailwag field is 10->25 gauss. The PFW's and spiller magnets (XS1 or XS2) are off during Flattop. The disadvantage in using the tailwag spill is that there is little control over the spill uniformity and the spill length is limited to 0.5->0.7 sec.

(b) Feedback spill.

The feedback spill is used primarily for higher Bevalac fields. The S1-Feedback spill allows external control of the extracted beam intensity (monitored by the F1-Scintillator, the Beam Fragment Detector (BFD), or an experimenter supplied signal) and increases the spill time to 1.0->1.7 sec. The PFW's are on during Flattop. At present the lowest Bevalac field for which optimized PFW's are available is 2.535 kG.

We do not distinguish between the two types of spills with the data presented here.

(4) Beam extraction radius (r_B).

The beam radius used for extraction is set at a value, with respect to the position of the thin septum of the XM1 magnet, which gives a growth per resonant period (3 turns) that is adequate to assure a good extraction efficiency. At present, the position of XM1 is set at a radius of 594.0", which results in the beam being extracted at a radius of around 601.5". The monitored beam radius r_B is calculated from the RF frequency and the Bevalac field, and represents an average radius in the machine. This in general is smaller (approx. 5"->1" for low to high Bevalac fields) than the beam radius at the XM1/XP1 magnets in the East Tangent Tank. At low fields we expect an increase in the extraction radius, to compensate for the larger beam size (less betatron damping).

If we look at the beam extraction radius used in past tunes, see Fig.10, we do not see any obvious correlation with the Bevalac field; however, there is a larger variation in the extraction radius at lower Bevalac fields. This may be due to extraction being less critically dependent on the beam radius for tailwag spill, which is usually used at low fields.

(5) Pole-Face-Windings (PFW).

The PFW's number 8 through 15 are used to shape the Bevalac radial guide field, and bring the betatron tune υ_x to the proper value for the 2/3 resonant extraction. Since the separatrix area depends on the perturbed tune, the PFW's will affect the Perturbation/Spiller magnet currents (XP1,XP2/XS1,XS2) used in extraction.

In Fig.16(a) to (h), we show the PFW current (Amp) dependence on the Bevalac field. The data comes from values used currently to extract beams at specific Bevalac fields, which have been optimized to give a good extraction efficiency.

The PFW8 and PFW15 are rarely used , have low currents (see Fig.16(a) and (h)), and their importance is not obvious. If we look at the dependence of the current in PFW9 on the Bevalac field, Fig.16(b), it shows a large current jump between 7 and 12 kG fields, which is difficult to interpret. These three PFW's (8,9,15) have no observable correlations with the other five (PFW10->14).

For the remaining PFW's (10->14), their most interesting feature is observed if we plot the correlations between them. It is sufficient to plot just four of them because the others show the same characteristics; so in Fig.17 (a) to (d) we have plotted PFW10,11,12 and 13 versus PFW14. We find that most of the PFW currents (I_{PFW}) lie on the linear curves shown, which pass through the origin. These correlations satisfy the simple relationship:

$$-3.33 \ I_{PFW10} = 3.48 \ I_{PFW11} = 2.29 \ I_{PFW12} = -0.97 \ I_{PFW13} = I_{PFW14} \quad (6)$$

To illustrate the effect of PFW's on the extraction optics, we compare two maximum Bevalac rigidity beams, extracted using the two sets of PFW currents listed below:

ACL name	"old PFW currents"	12575EXT
PFW # 8	0.5 (amp)	0.0 (amp)
9	0.1	-1.9
10	67.7	21.7
11	-34.6	-20.7
12	-25.6	-31.7
13	-2.7	74.5
14	0.0	-72.5
15	-0.5	0.0

The PFW currents used for 12.575 kG Bevalac field extraction prior to 1990, are listed in column 2 ("old PFW currents"). Their values are not consistent with the correlation ratios of Eqn.(6), except for PFW13/PFW14.

The presently used set of PFW currents , with ACL name 12575EXT, are listed in column 3, and are consistent with all the correlation ratios of Eqn.(6). They also have a significant effect on the beam emittance. For TUNE 81, they were used to extract 12.575 kG protons. In table TUNE 81A, we give the magnet currents, wire chamber beam intensity profiles, and a polaroid exposure of the beam at the Q3-Scintillator location. From this, the best fit beam parameters were calculated and the optics program LATTICE[4] (table TUNE 81B gives the transport list) was used to calculate the beam envelope, which is shown in Fig.5.

In comparison, in Fig.6, we show the beam envelope for

TUNE 66 which had the same XP1 current (175 amp), but used the old PFW currents (column 2). Comparing the two, the extraction efficiency was about the same (40 to 30%), but the beam emittance was significantly lower for TUNE 81 than for TUNE 66 (see also Fig.13):

TUNE	E_x	E_y	
81	6.3	1.8	π mm-mr
66	16.1	12.6	

(6) Perturbation/Spiller magnets XP1,XP2/XS1,XS2.

The time-independent perturbation magnets XP1 and XP2 excite a mainly sextupole field to produce an unstable fixed point adjacent (4->8 cm)[3] to the beam closed orbit radius, see Fig4. Idealy the beam should lie inside the stable-orbit separatrix area (typically 100 π mm-mr)[3] at the start of extraction. The second perturbation magnet XP2 was designed[1] to be used together with XP1 to improve the extraction efficiency for low Bevalac fields.

If we extract the beam with the tailwag method, then the Bevalac field is ramped to move the beam gradually across the unstable fixed point, producing a growth in the radial betatron ampitude and causing the ions to cross the XM1 magnet septum. The dipole extraction magnets XM1,XM2 and XM3 then transport the captured beam out of the machine, as shown in Fig.3.

With the feedback spill method of extraction, the spiller magnet XS1 or XS2 (both mainly sextapole) is ramped, shrinking the separatrix area, moving the unstable fixed point across the beam resulting in extraction. The ramp signal establishes an approximate rate of spill, while a feedback signal maintains the spill at the desired rate. For the beam to jump the XM1 septum, the radial speed of the unstable fixed point should be about 4->8 cm/sec[3]. The XS1 spiller was designed to extract beam at high fields, and XS2 for low fields[1].

Because of an XM1 current limit at high Bevalac fields, at present the polarity of the XP1 perturbation magnet is opposite to that used in the design report[1], so that the 2/3 resonance is approached from above during extraction.

The dependence of the XP1 and XP2 currents/Bevalac field on the Bevalac field is shown in Fig.18 and Fig.19 respectively.

If we select only the 12.575 kG tunes, all of which used the standard 12575EXT PFW's (except TUNE 81), and plot the horizontal beam size at XM3WC as a function of the XP1 current, see Fig.15 (a), we observe that the size increases with increasing current. At the F1 focal point, this was observed as an increase in the beam divergence (about 1 mr) but not the beam size. The range of XP1 currents (120->210 amp/kG) indicates that there is a broad region where the extraction efficiency is adequate.

(7) Dipole magnet XM1.

The XM1 magnet current is set by the requirement that the beam be centered horizontally on wire 16.5 at XM2WC. Its current dependence on the Bevalac field is shown in Fig.20. Because the XP1 magnet steers the beam, it affects the choice of XM1 current. We find, as shown in Fig.21, that higher XP1 currents require lower XM1 currents. The correlation between XP2 (same polarity as XP1) and XM1 is less obvious (see Fig.22).

(8) Dipole magnets XM2.

The XM2 magnet is normally placed at a standard radial position of 586.5".

In the tunes studied here, the current in XM2 has been set so as to center the beam horizontally near wire 20 at XM3WC. The significance of the horizontal beam position on XM3WC is discussed in Sec.10.

From Fig.23, it appears that the dependance of the XM2 current/Bevalac field on the Bevalac field is quite linear.

(9) Dipole magnet XM3.

The XM3 magnet current is set so as to center the beam horizontally on wire 16.5 at XM4WC. The dependence of the XM3 current/Bevalac field on the Bevalac field is shown in Fig.24 and is approximately quadratic.

A dipole magnet will bend a beam of rigidity R_B by the

angle:

$$\emptyset_M = (B_M\, L_{eff})/\, R_B \tag{7}$$

where L_{eff} = effective beam path-length in magnet

$$= \int B\ dl/B_M$$

B_M = peak magnetic field in magnet

The beam bend angle in a dipole magnet is therefore proportional to the magnet current/Bevalac field (for no magnet saturation). From Fig.23 and Fig.24, we observe that the bend angle through both XM2 and XM3 magnets decreases with increasing Bevalac field. Specifically, the conversion factor to calculate the bend angle is $9.38\ 10^{-3}$ deg/(amp/kG) for XM2, and $2.96\ 10^{-2}$ deg/(amp/kG) for XM3. For XM3, we find that the bend angle changes from about 6.3 deg. at a Bevalac field of 2 kG, to about 4.5 deg. at a full field of 12.575 kG.

(10) Beam at XM3WC.

The horizontal beam size at XM3WC increases with the Bevalac field as shown in Fig.15(b). At full field it can fill up the XQ3A aperture (4.4" diameter), and therefore requires that the beam be properly positioned on XM3WC. For a Bevalac field of 12.575 kG (TUNE 66: $^4He^{2+}$), centering the beam horizontally on wire 23 at XM3WC[5] and wire 16.5 at XM4WC, gave negligible XQ3 quadrupole steering (with XQ3 off, the beam direction changed by 0.3 mr) and the beam was centered in the XQ3A aperture (observed with a polaroid at the Q3-Scintillator position). At low Bevalac fields (2 kG) the horizontal beam size is smaller by about a factor of two, so beam clipping should not occur for properly centered beams. The observed difference in XM3 bend angle (Sec.9) indicates (neglecting XQ3 quadrupole steering) that the beam differs in entrance angle by about 1.8°. So to obtain the same exit conditions as in TUNE 66, we would have to center the low field beam about 2.6 cm (9 wires) to the left of the high field position (wire 23) on XM3WC.

If we look at the vertical beam size at XM3WC, we find that it decreases with the Bevalac field as shown in Fig.15(c). At low fields (2 kG) the beam has about a 2" diameter, which is five times larger then that at high fields. Since the XM3 vertical pole-tip aperture is 2", we expect beam clipping at low fields. This beam loss

will come from the upper (top) part of the beam, because the extracted beam at XM3WC is about 1.5 cm high (1.0 cm for high fields).

(11) Quadrupole doublet XQ3A and XQ3B.

In this quadrupole doublet, XQ3A is horizontally focusing and XQ3B is vertically focusing. They are tuned by the MCR operators to produce a horizontal and vertical focus (waist) at wire chamber XF1WC, the first focal point (F1) out of the machine.

The dependence of the quadrupole currents (normalized to the Bevalac field) on the Bevalac field is shown in Fig.25(a) and (b) for XQ3A and XQ3B respectively. We observe that the focusing strengths in both quadrupoles exhibit a rapid increase of about 40%, around a Bevalac field of 4 kG. In addition, the XQ3A/XQ3B current ratio (see Fig.25(c)) does not remain the same, but decreases by about 10%, again at a field near 4 kG.

These changes in quadrupole focusing strength are due to changing beam extraction optics. We will look at this in terms of the location of the last horizontal (F_{0x}) and vertical (F_{0y}) focal points (real or virtual) inside the machine (upstream of XQ3). Using the XQ3 currents and magnet dimensions, we calculated the Transport matrix for the quadrupole doublet. Making the approximation that the downstream focal point F1 is at XF1WC (5.38 m downstream from the center of XQ3), we calculated from the Transport matrix the positions of horizontal (F_{0x}) and vertical (F_{0y}) focal points with respect to XM3WC (2.56 m upstream from the center of XQ3). They are shown in Fig.26(a) and (b). We observe that the upstream horizontal focal point F_{0x} moves closer to XM3WC (and XQ3) with increasing field, as might be expected from the increase in quadrupole strength. The upstream vertical focal point F_{0y} appears to have two preferred positions: one about 7.5 m downstream of XQ3 for low fields (1.5->4 kG), and the other about the same distance upstream for high fields (4->12.575 kG). At high Bevalac fields the horizontal and vertical focal points are at approximately the same location, about 5 m upstream of XM3WC. As the Bevalac field decreases, the focal points split. At a 2 kG field, the horizontal focal point F_{0x} is about 15 m upstream of the XM3WC, while the

vertical one F_{0y} is about 10 m downstream (in the area of XF1WC).

Using average (approx.) beam and magnet values, we show a typical low Bevalac field (2 kG) beam envelope in Fig.7, which can be compared with a typical beam envelope at a high Bevalac field (12.575 kG) shown in Fig.8. They illustrate the changes in beam optics that have been discussed here, as we go from low to high Bevalac fields.

----

(1) "High intensity Uranium beams from the SuperHilac and the Bevatron", LBL-14881,March 1982.

(2) J.G.Kalnins, " Beam Phase-space Parameters at the SuperHilac Exit", October 7,1988, LBL (unpublished).

(3) J.Staples, "Cause and Cure of Extracted Beam Modulation at the Bevatron", May 26,1988,LBL (unpublished).

(4) J.Staples, " LATTICE ... A Beam Transport Program", June 1987 (revised September 1988, August 1989), LBL-23939.

TUNE 81A: Magnet currents and beam sizes for TUNE 81.

Protons at a Bevalac field of 12.575 kG
Beam extraction radius = 599.6"

Magnet		Current	
XP1	SP	174.00	amp
XP2	SP	0.00	
XM1	AM	1198.75	
XM2	AM	2299.51	
XM3	AM	1894.42	
XQ3A	AM	1343.43	
XQ3B	AM	1458.23	
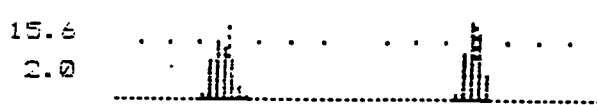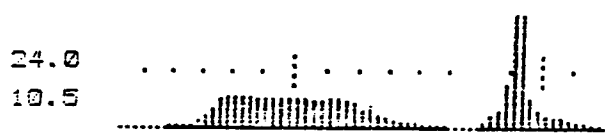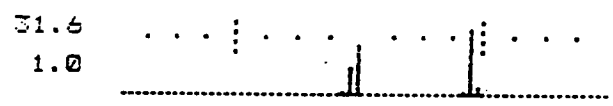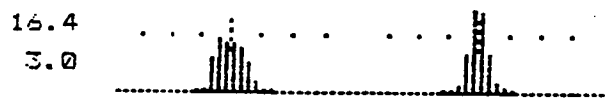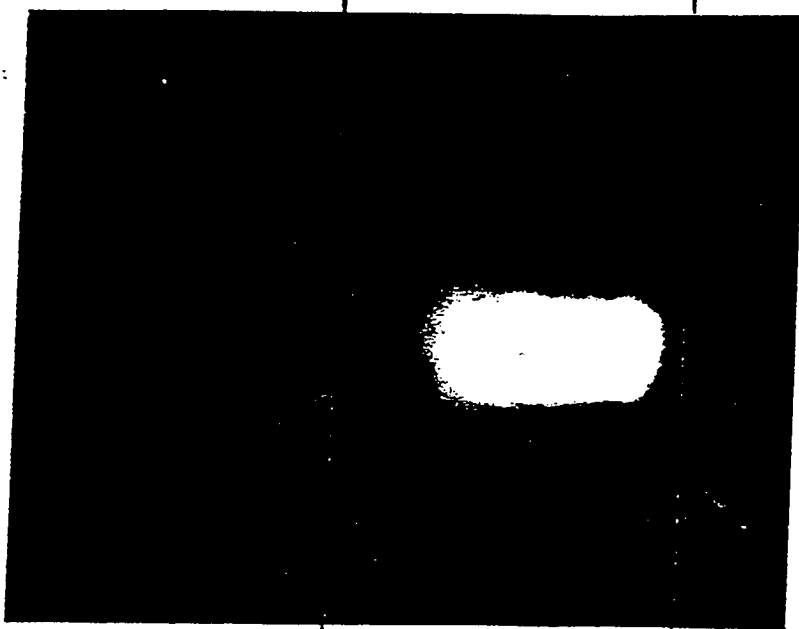
Beam size
on a polaroid
of P3-Scint.
(full scale, looking
downstream)

3 pulses

TUNE 81B: Transport element list.

```
Beam rigidity =     19.2000 t-m
x,y emittance =      0.6330    0.1824 cm-mrad
dp/p =  0.000%

Transport mode
        betax =    51.0858    alphax =     9.2639
        betay =    79.1845    alphay =    12.3479
        etax  =     0.0000    eta'x  =     0.0000
        etay  =     0.0000    eta'y  =     0.0000
```

	name	type	vcode	lth,angle	b,b',s	n,gap	xaper	yaper
1	xm4wc	lens	0.0	0.000000	0.000000	0.0000		
2	l2	drift	0.0	0.230000	0.000000	0.0000		
3	xq4b	quad	0.0	0.884000	0.000000	0.0000	0.1000	0.1000
4	s1	drift	0.0	0.284000	0.000000	0.0000		
5	xq4a	quad	0.0	0.884000	0.000000	0.0000	0.1000	0.1000
6	l1	drift	0.0	3.969000	0.000000	0.0000		
7	xflwc	lens	0.0	0.000000	0.000000	0.0000		
8	d1	drift	0.0	4.351000	0.000000	0.0000		
9	xq3wc	lens	0.0	0.000000	0.000000	0.0000		
10	d2	drift	0.0	0.209000	0.000000	0.0000		
11	xq3b	quad	2.2	0.788000	-20.896000	0.0000	0.0559	0.0559
12	t1	drift	0.0	0.076000	0.000000	0.0000		
13	xq3a	quad	1.2	0.788000	19.250999	0.0000	0.0559	0.0559
14	d3	drift	0.0	0.195000	0.000000	0.0000		
15	xm3e	edge	0.0	2.230000	1.062900	0.0000	0.0635	0.0254
16	xm3	bend	0.0	1.406000	-1.062900	0.0000	0.0635	0.0254
17	xm3e	edge	0.0	2.230000	1.062900	0.0000	0.0635	0.0254
18	d4	drift	0.0	0.135000	0.000000	0.0000		
19	xm3wc	lens	0.0	0.000000	0.000000	0.0000		
20	d5a	drift	0.0	5.801000	0.000000	0.0000		
21	d5b	drift	0.0	5.000000	0.000000	0.0000		
22	bev	lens	0.0	0.000000	0.000000	0.0000		

where

lth = effective length (m)
b' = quadrupole gradient (T/m)
b = bend magnet field (T)
angle = bend magnet edge angle (deg)
xaper,yaper = horizontal,vertical half-apertures (m)
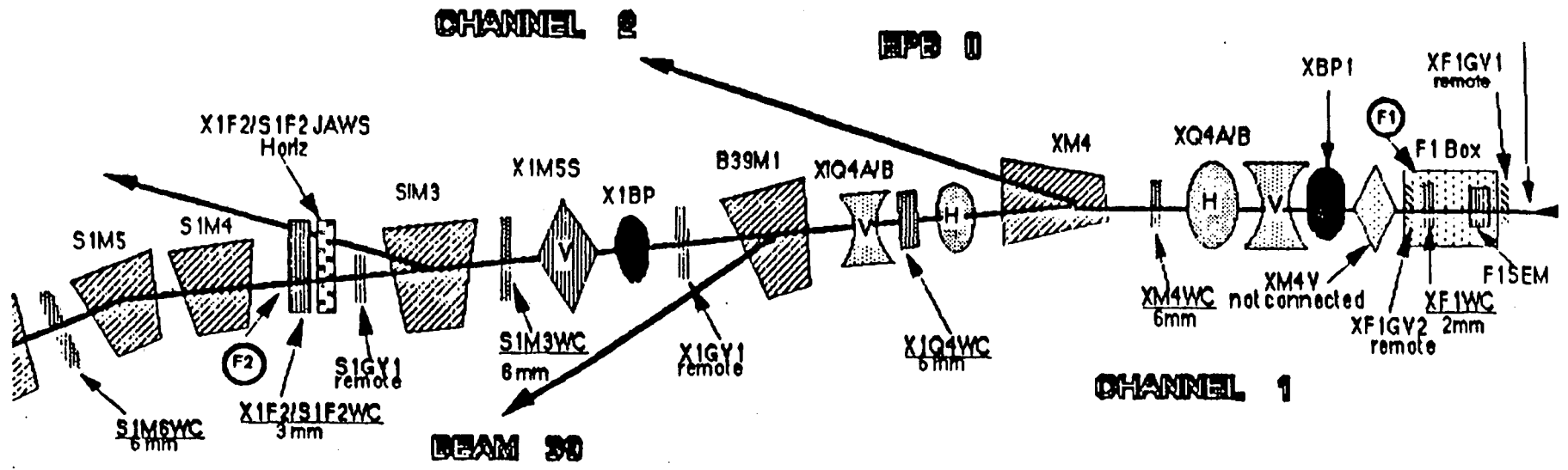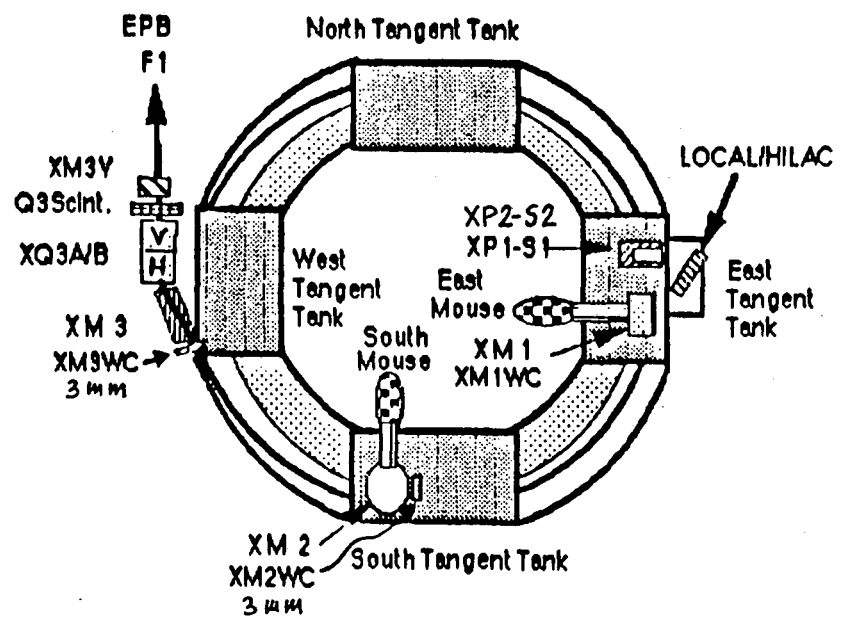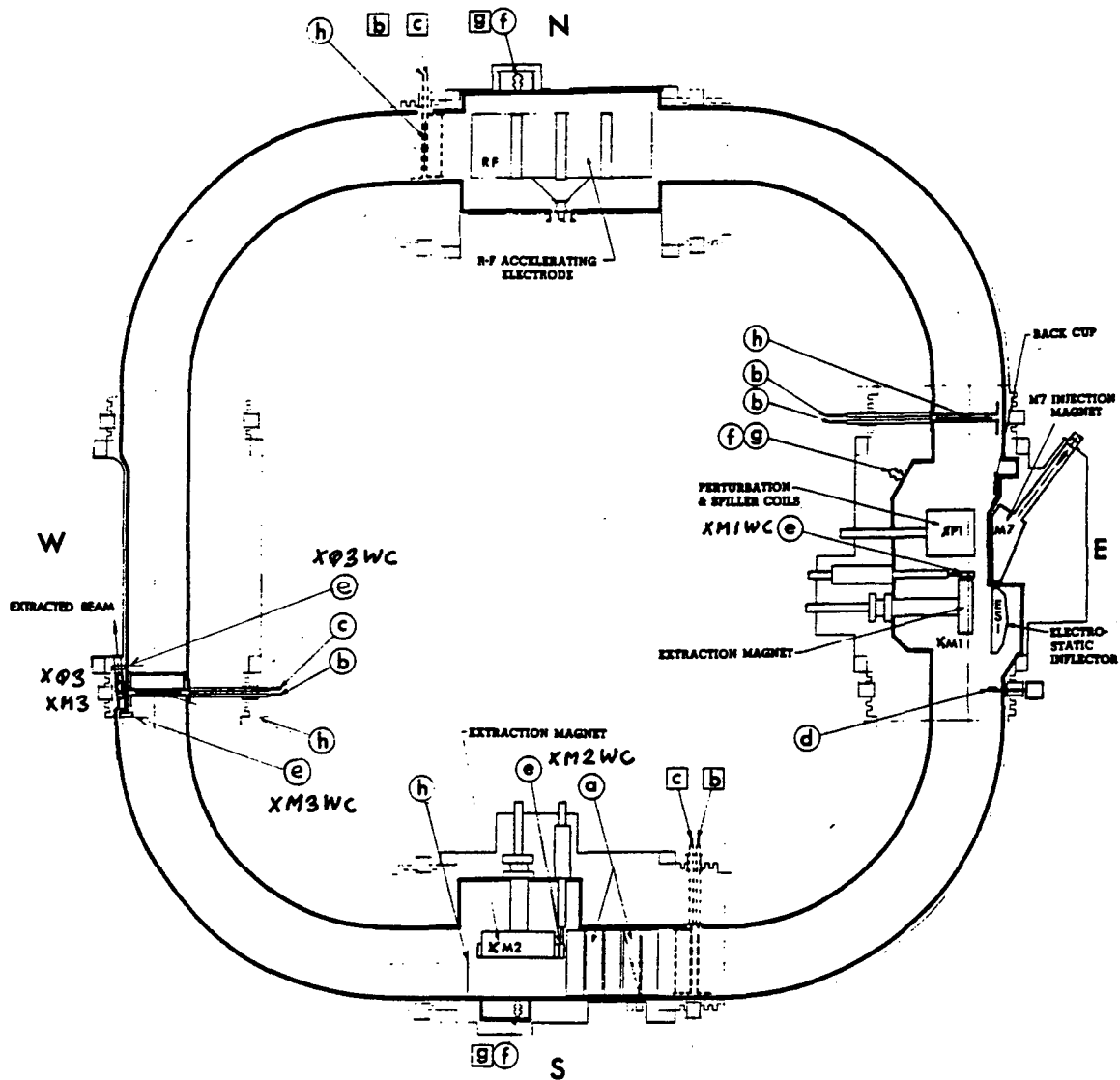
Figure 1

Figure 2 . Bevatron beam instrumentation (XBL 827-10672).

a. Beam induction electrode   e. Multi-wire chambers
b. Finger probes   f. Ion gauges
c. Vertical clippers   g. Residual gas analyzer
d. Inflector (E.O.S.) cup   h. Fixed beam scraper

15

Resonant extraction scheme for the Bevatron

Note: The particle motion shown as a sinusoidal motion with $\nu_R = 2/3$ gives a somewhat simplified picture.

XBL 731 19

Fig.3

Radial phase diagram of 2/3 integral resonance
excited for extraction at east straight section.

Fig.4

Fig.5: TUNE81 12.575 kG 1H1+ with PFW=5666EXT
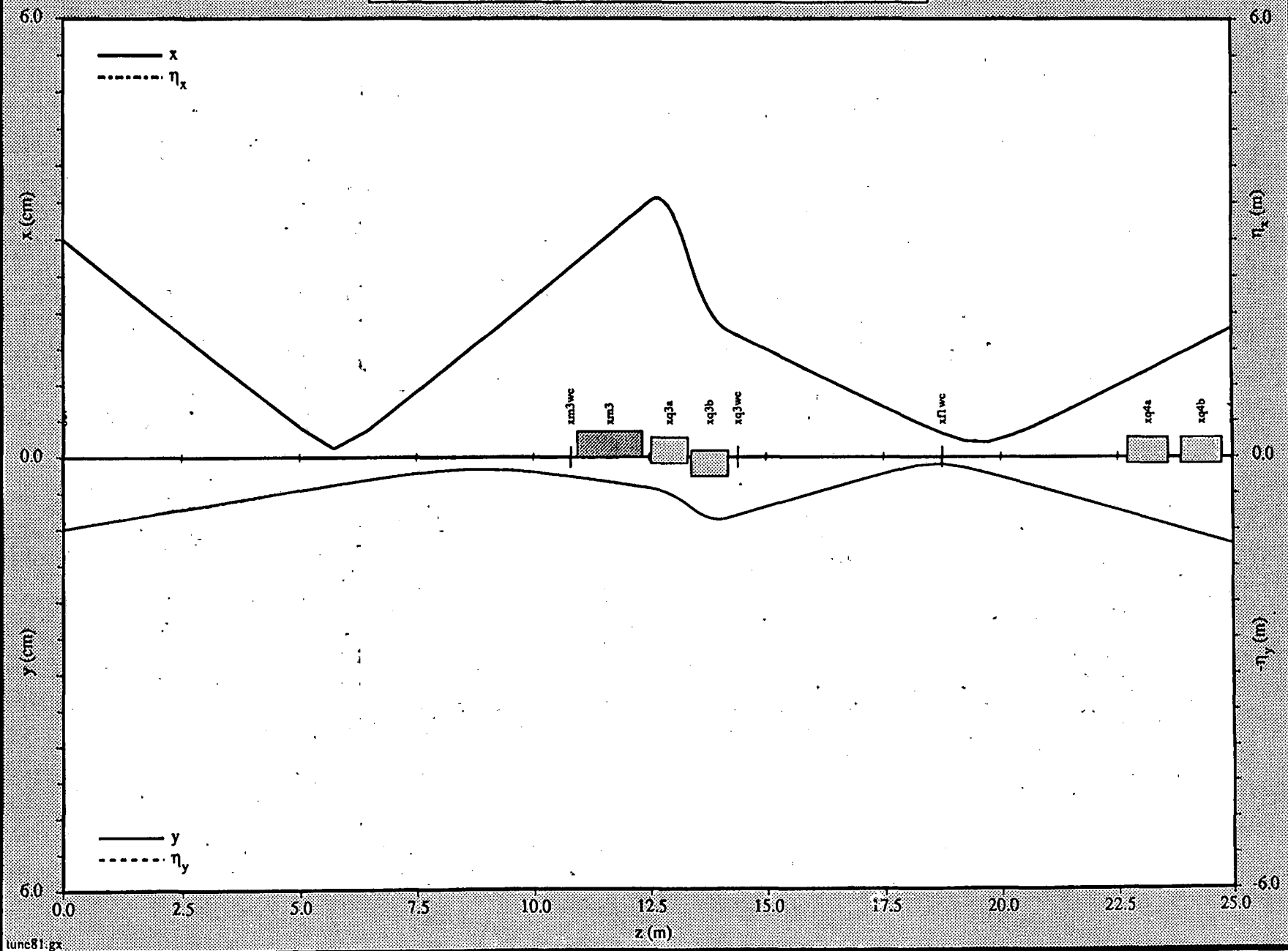
Fig.6: TUNE66 12.575 kG 4He2+ with PFW=12575EXT

Fig.7: Typical beam envelope for low (1.5->4 kG) Bev field
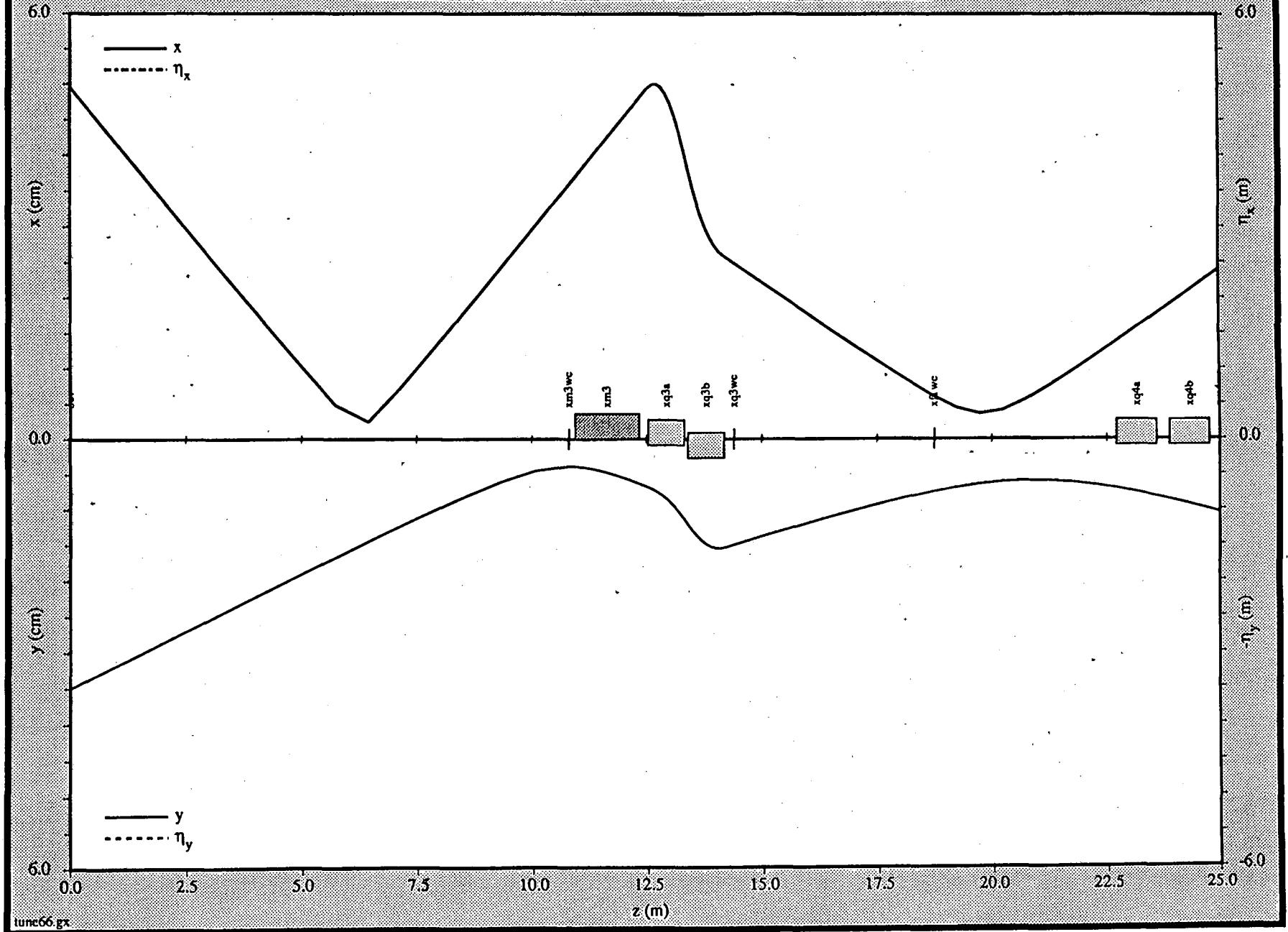
Fig.8: Typical beam envelope for high (4->12.575 kG) Bev field

21
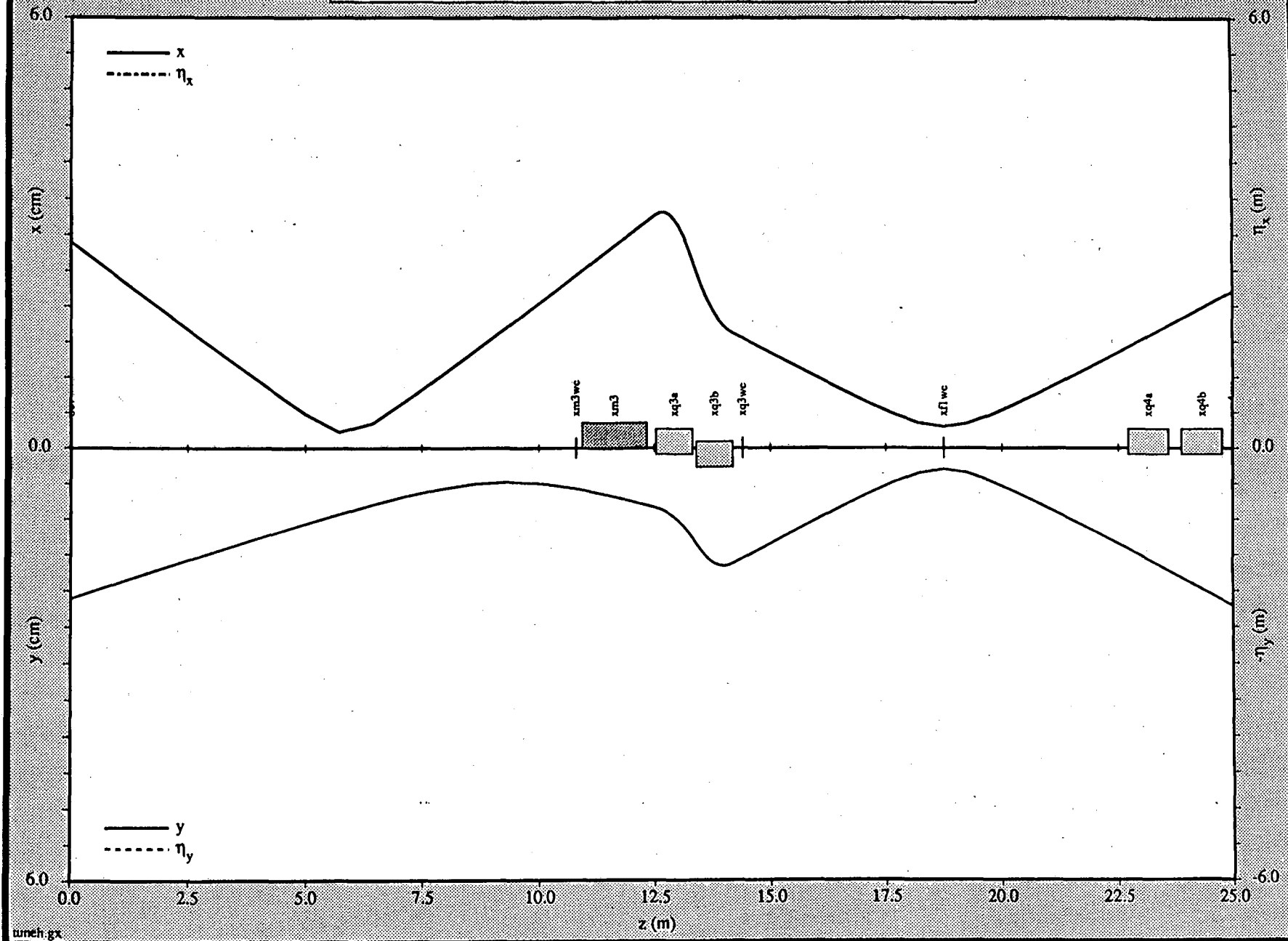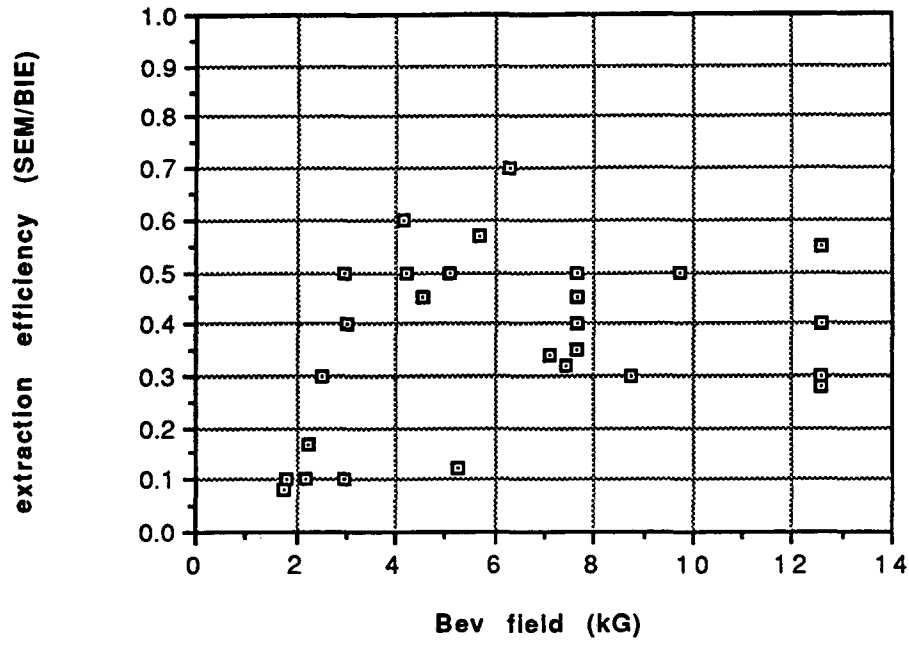
Fig.9
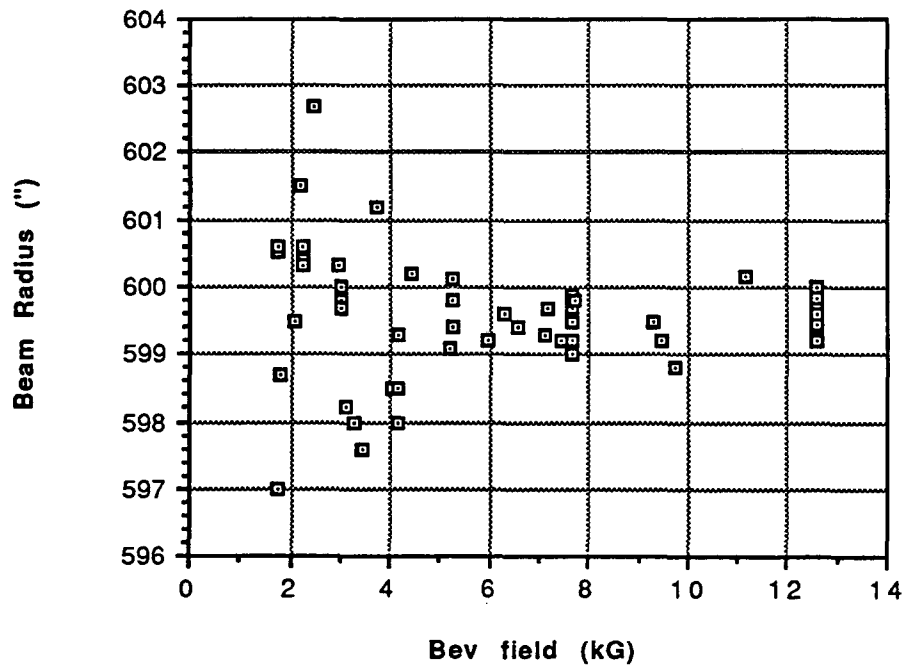
Fig.10
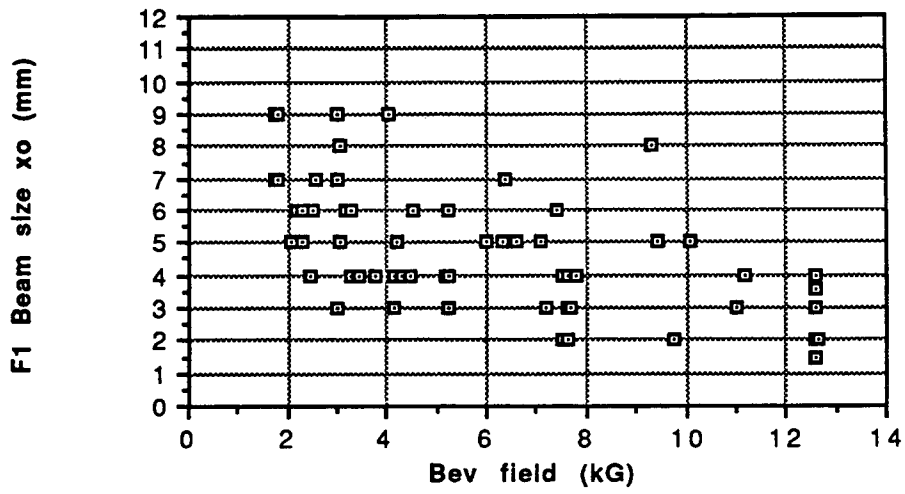
Fig.11(a)

Fig.11(b)

Fig.11(c)

23
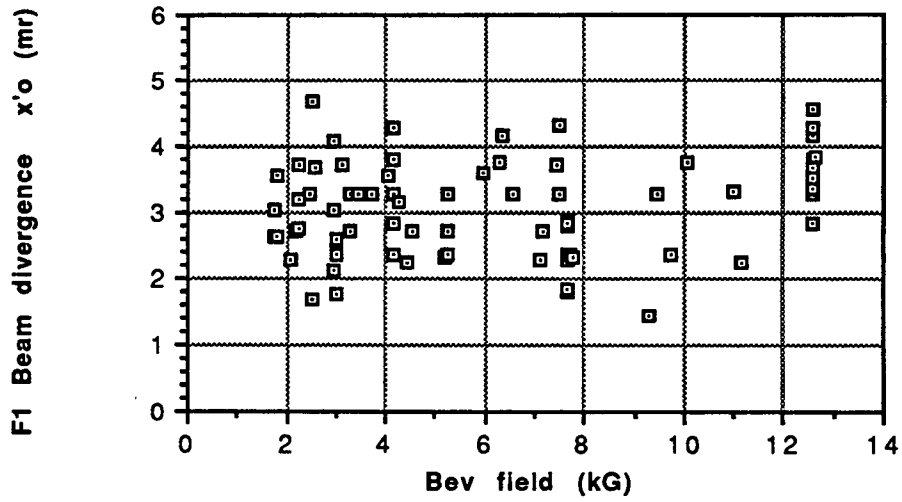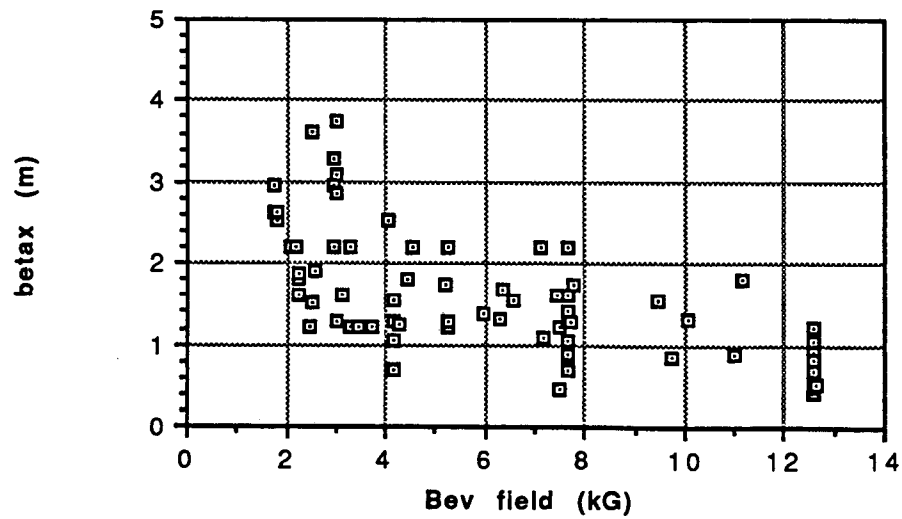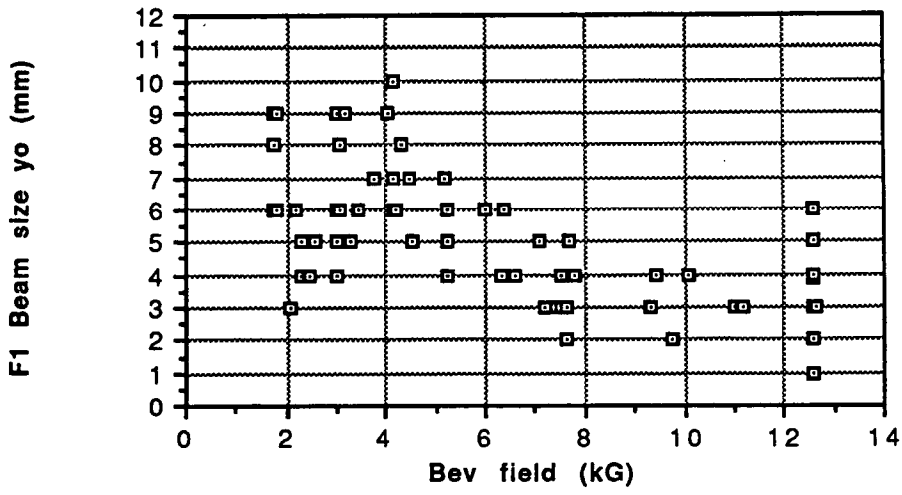
Fig.12(a)

Fig.12(b)

Fig.12(c)

24
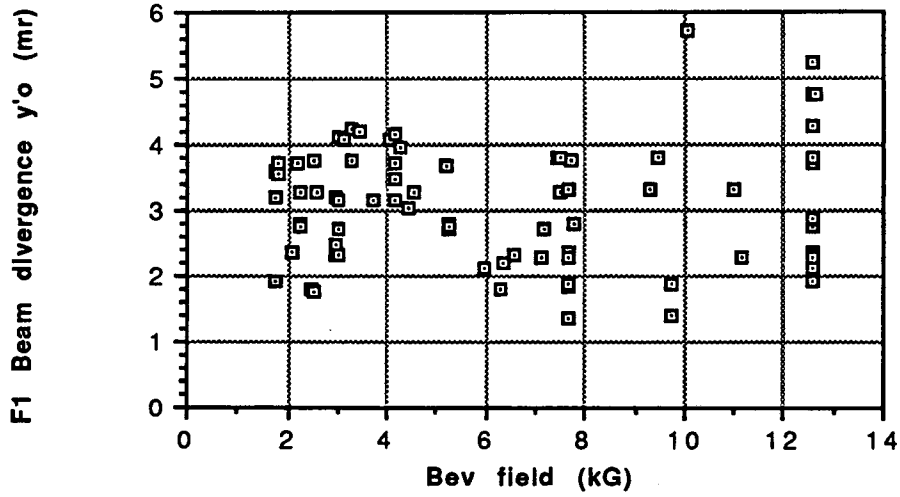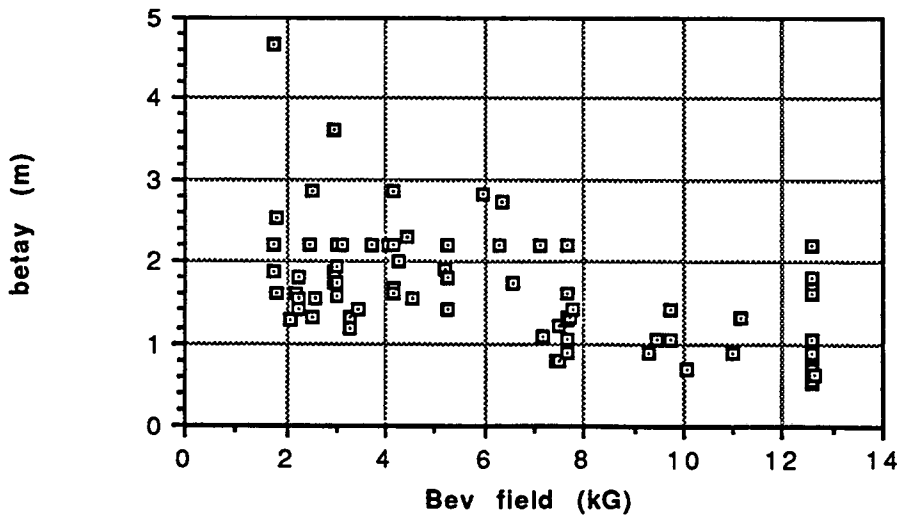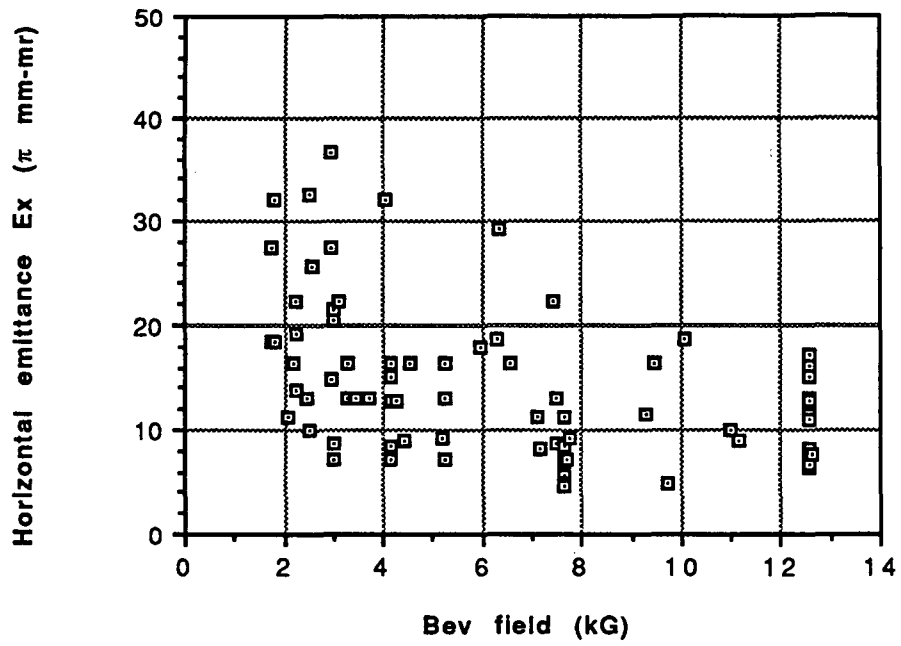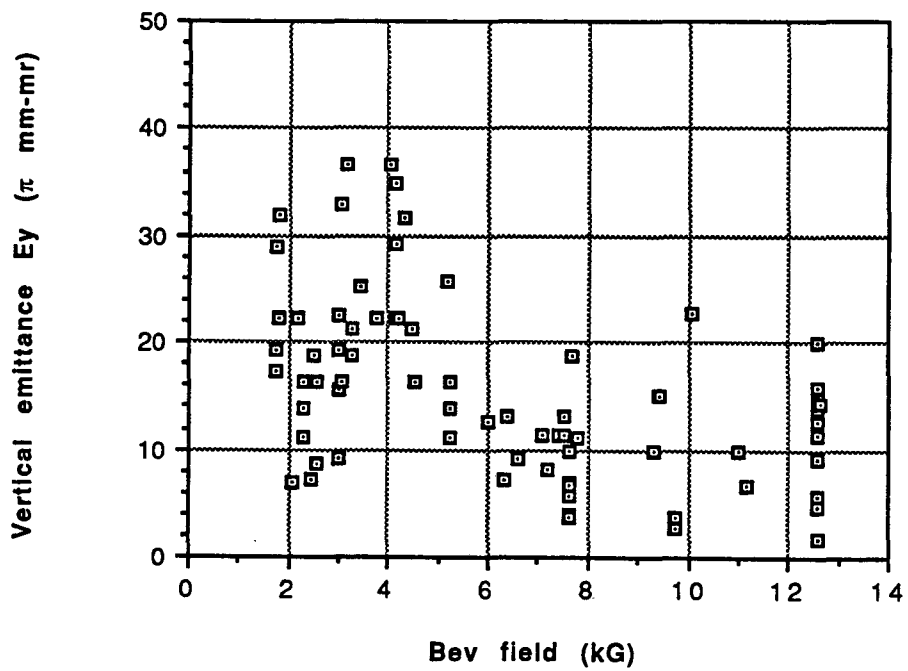
Fig.13(a)

Fig.13(b)
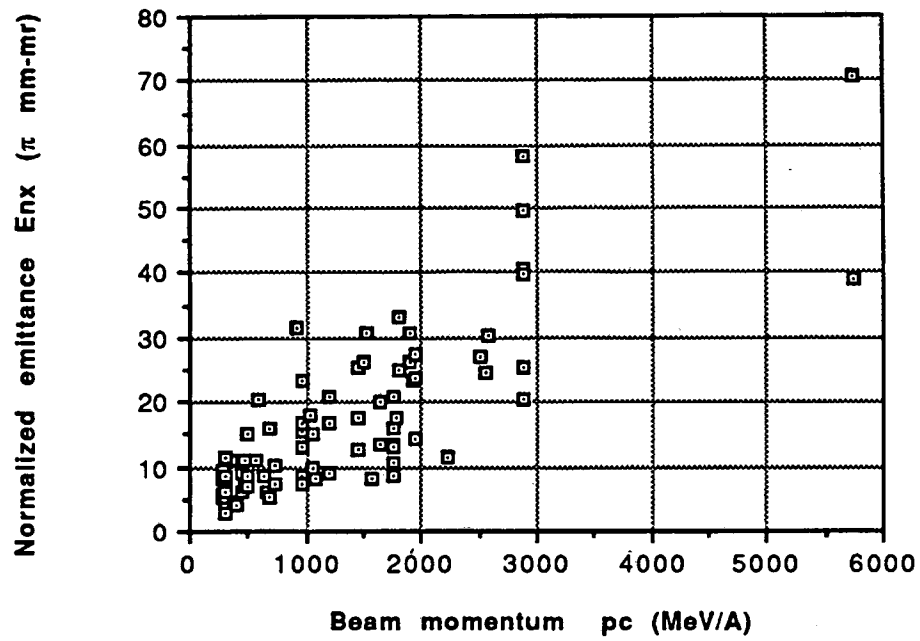
Fig.14(a)
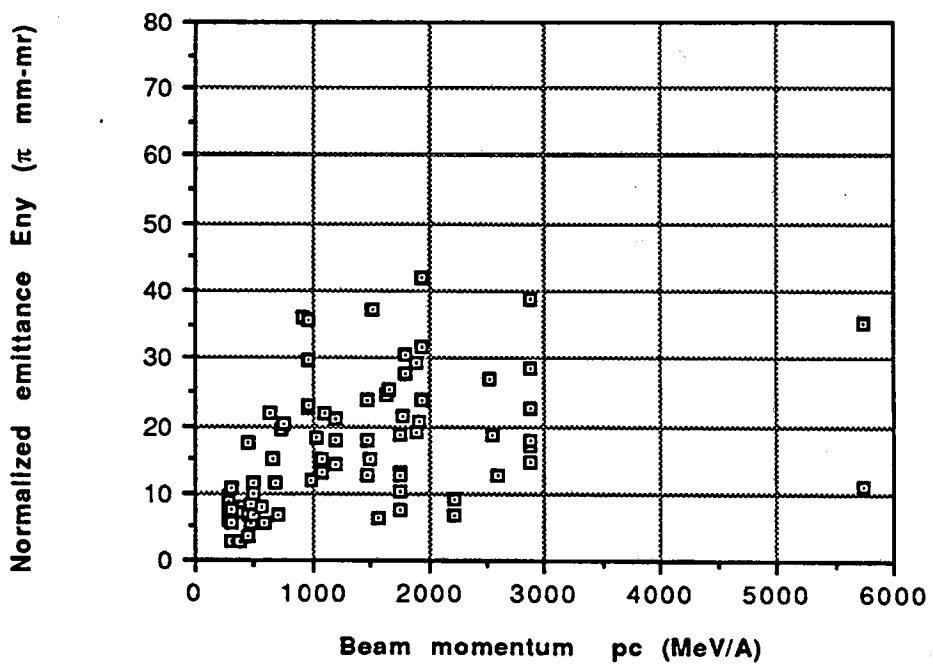
Fig.14(b)
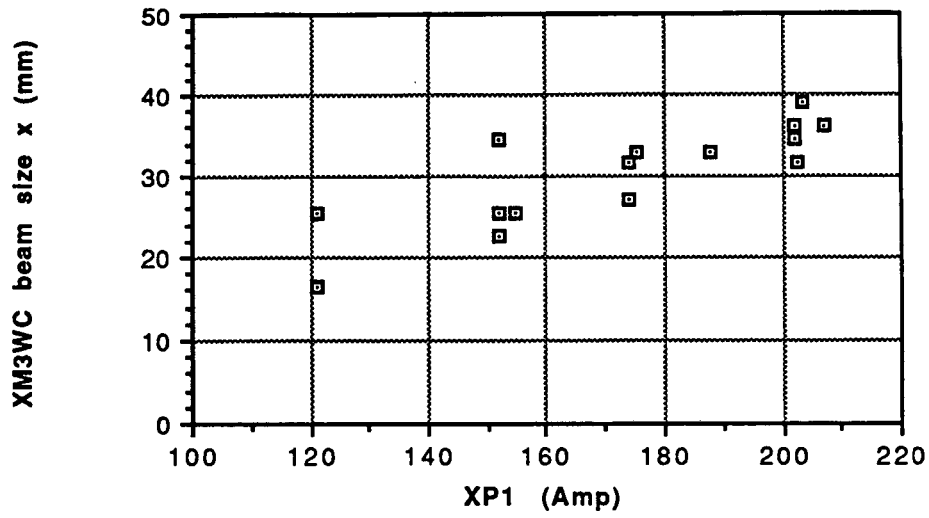
Fig.15(a)

Bevalac field = 12.575 kG

Fig.15(b)

Fig.15(c)

27

Fig.16(a)

Fig.16(b)

Fig.16(c)

28
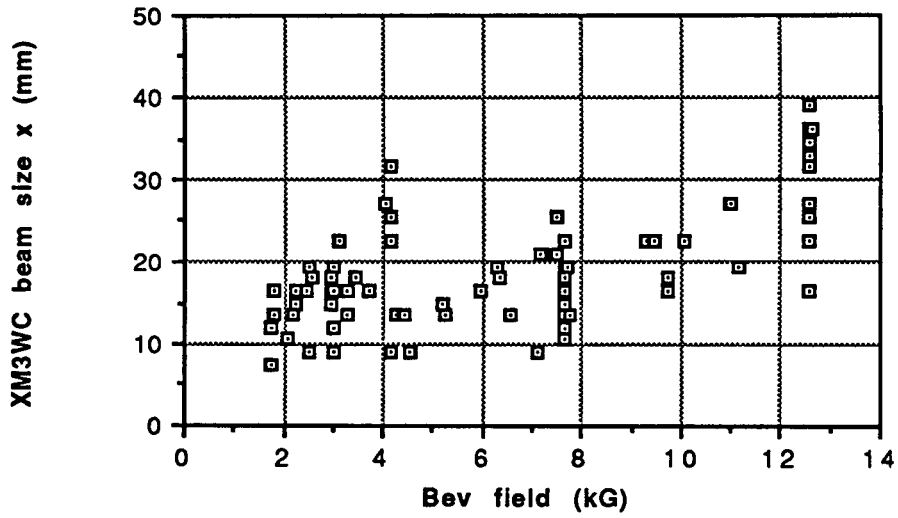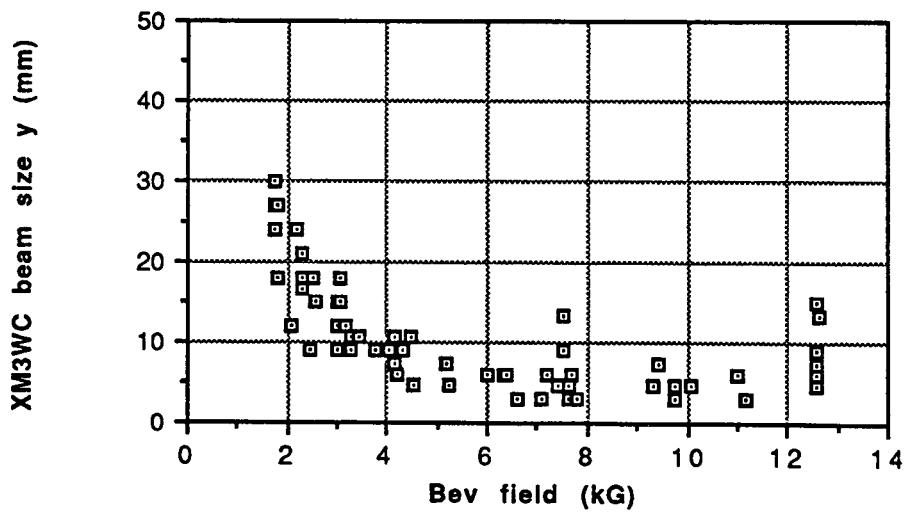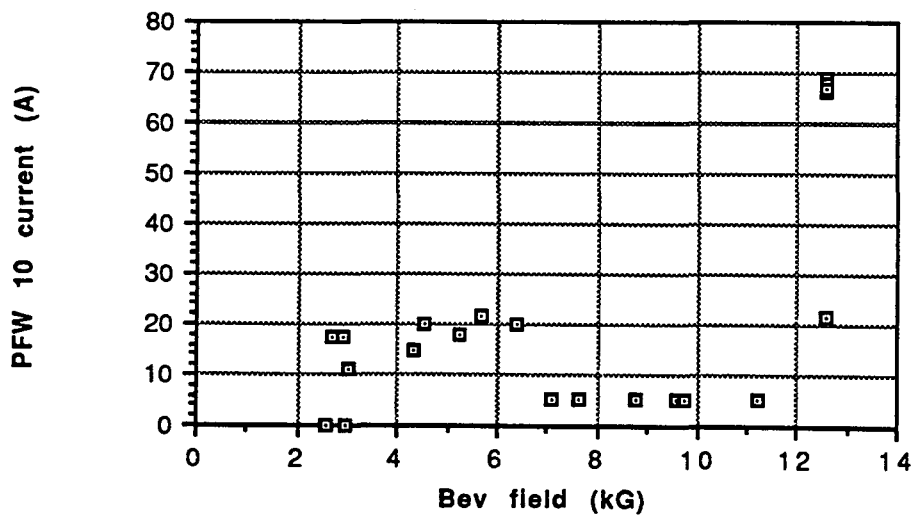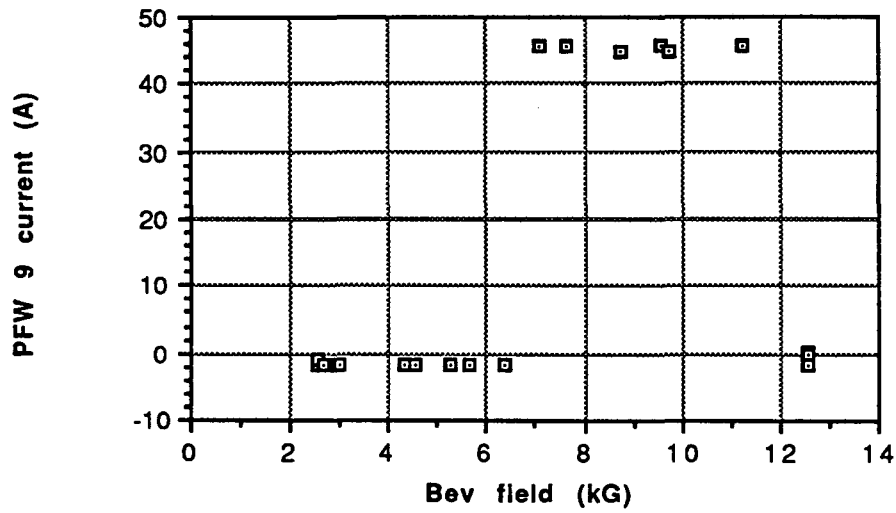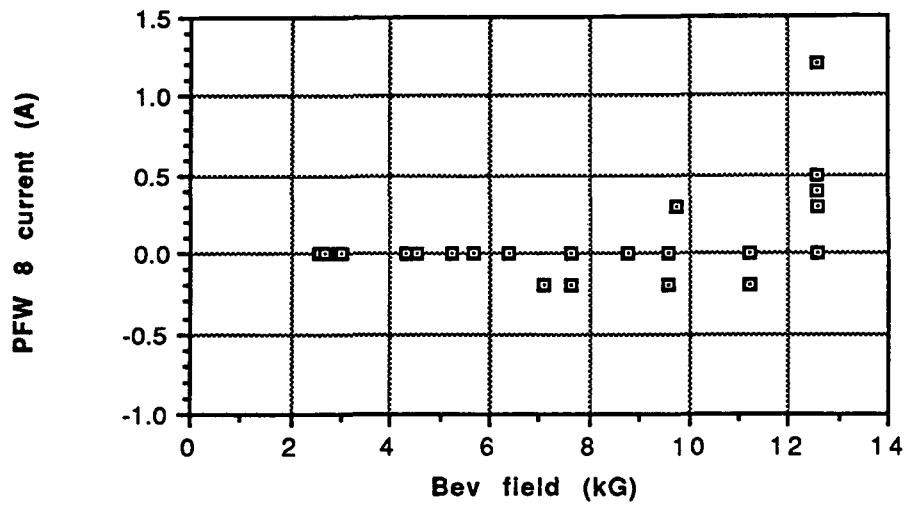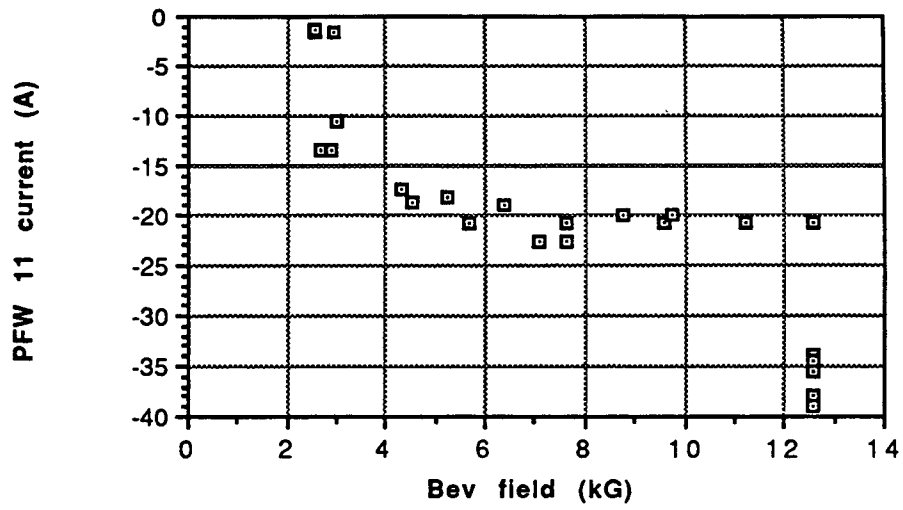
Fig.16(d)

Fig.16(e)

Fig.16(f)

29
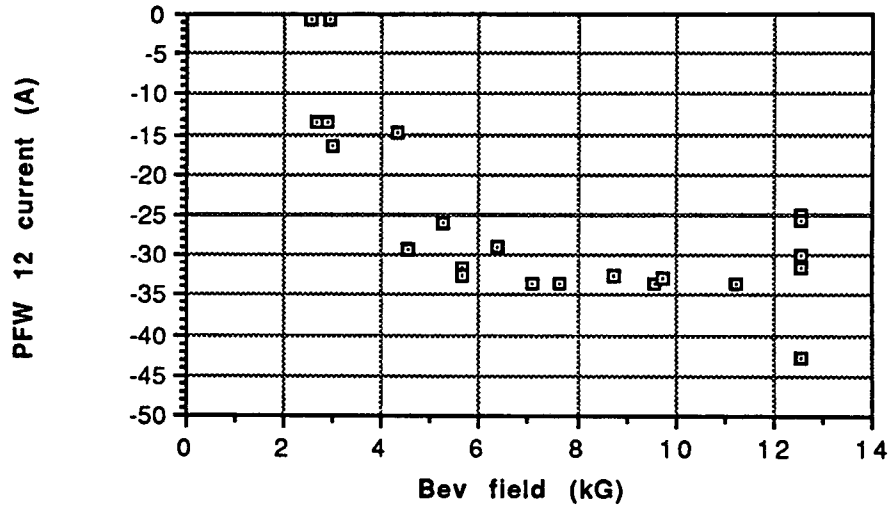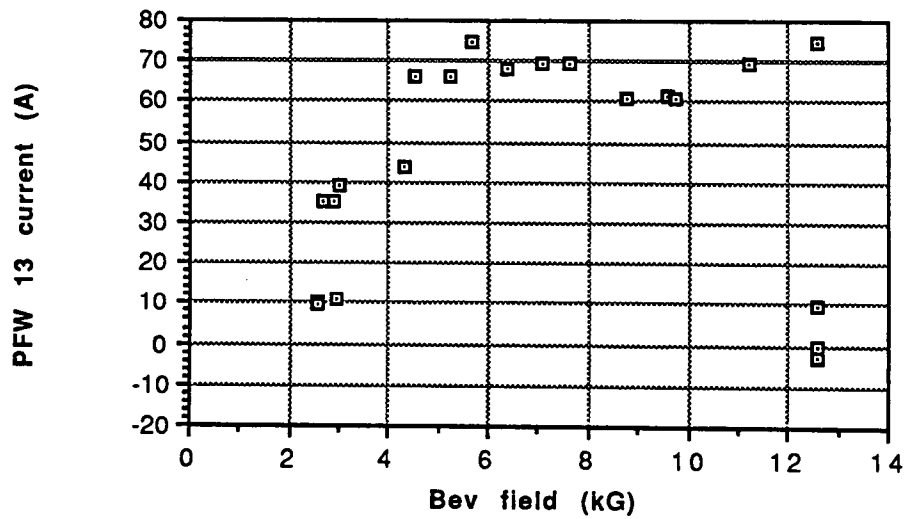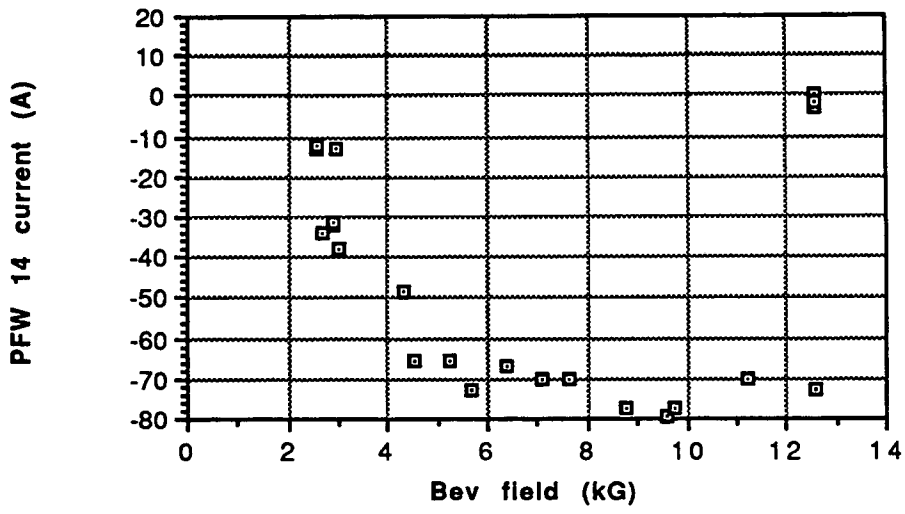
Fig.16(g)

Fig.16(h)

Fig.17(a)

30
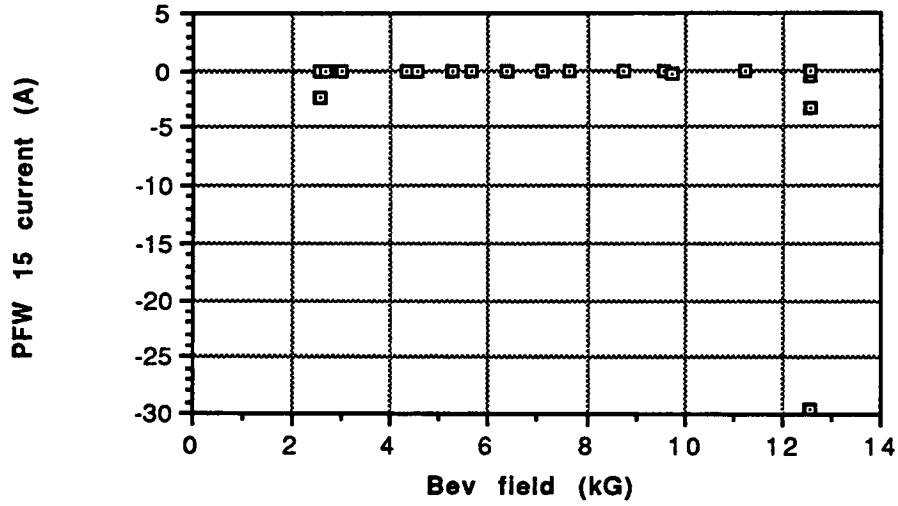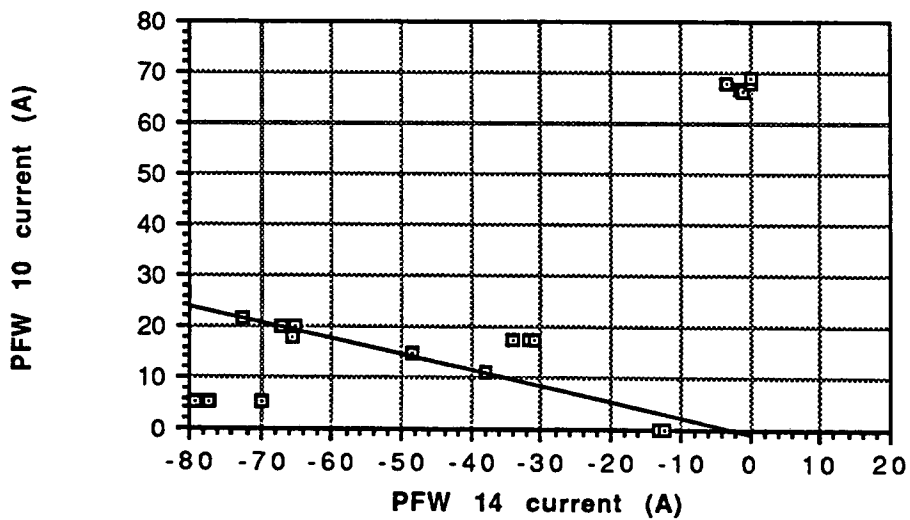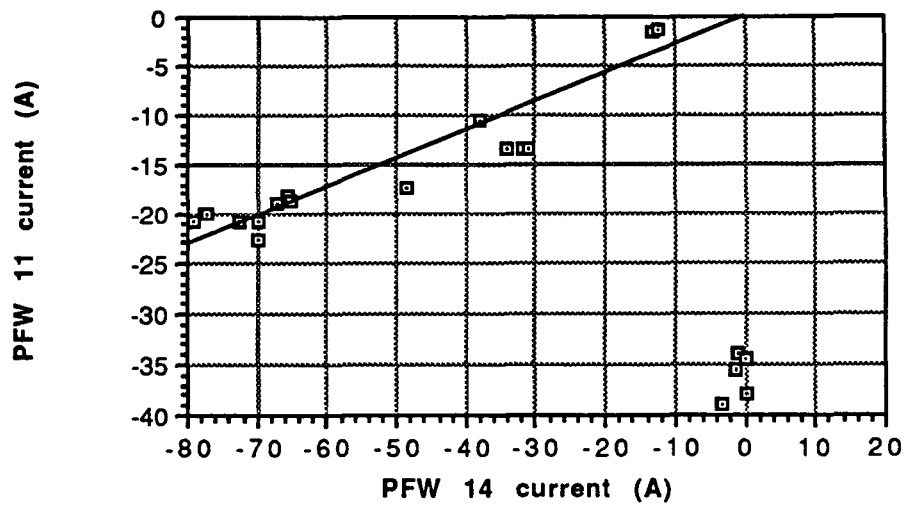
Fig.17(b)

Fig.17(c)

Fig.17(d)

31

Fig.18

Fig.19

Fig.20

32
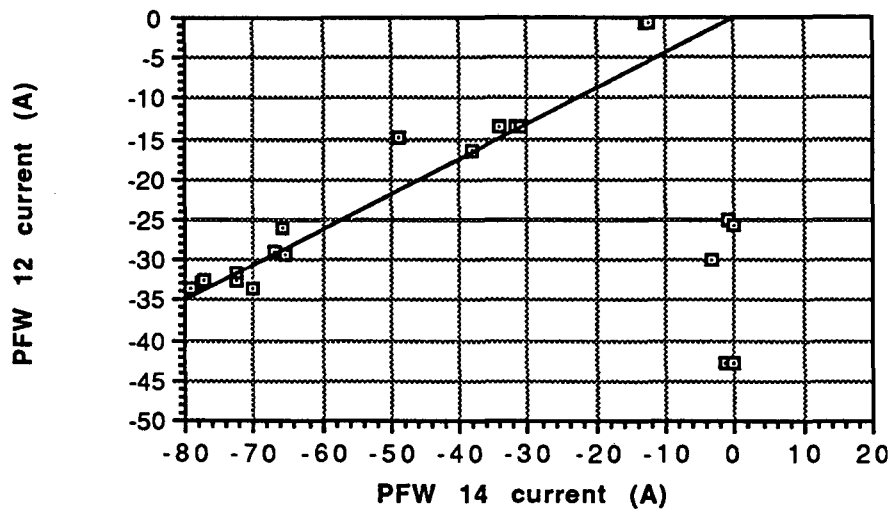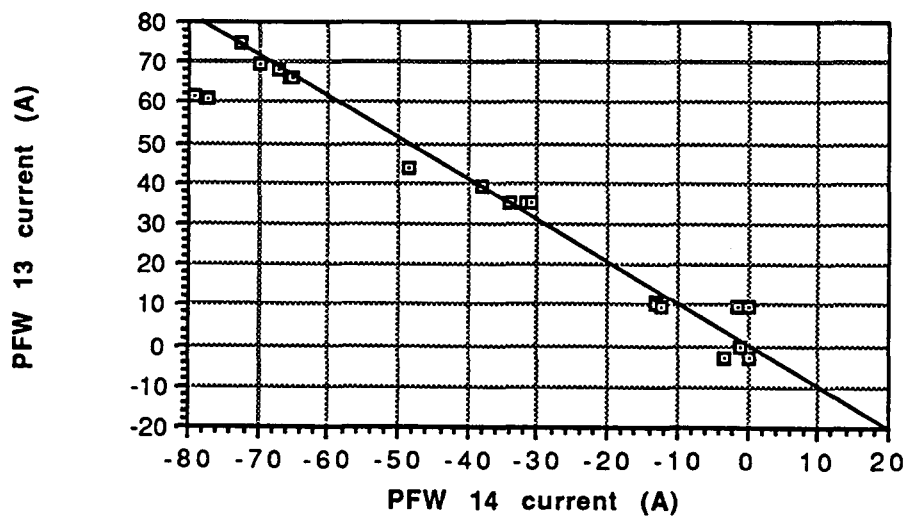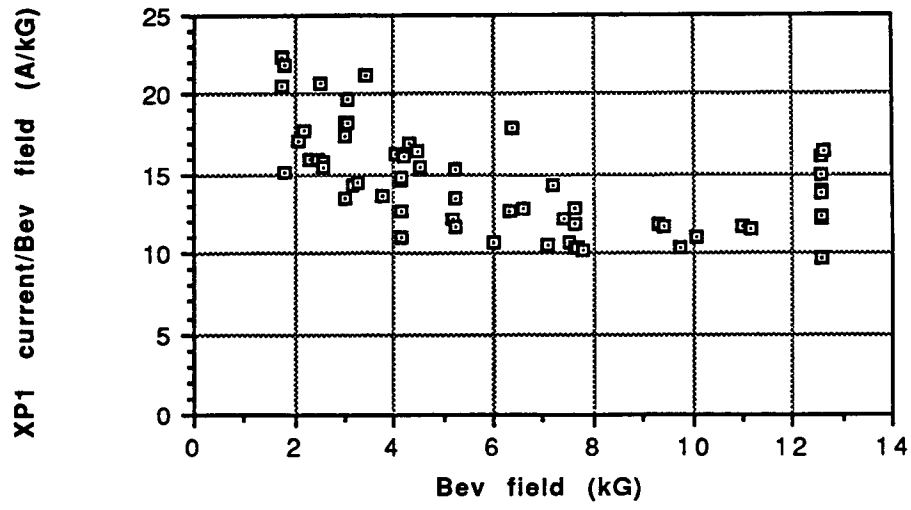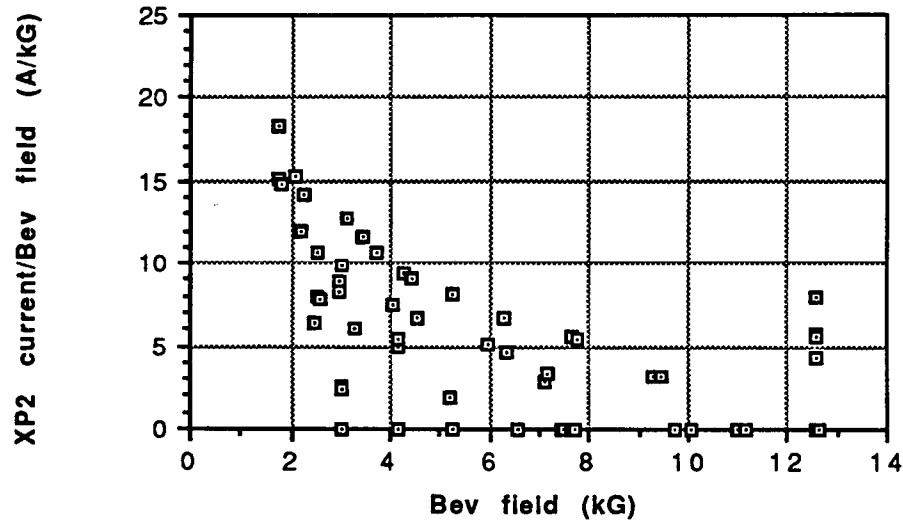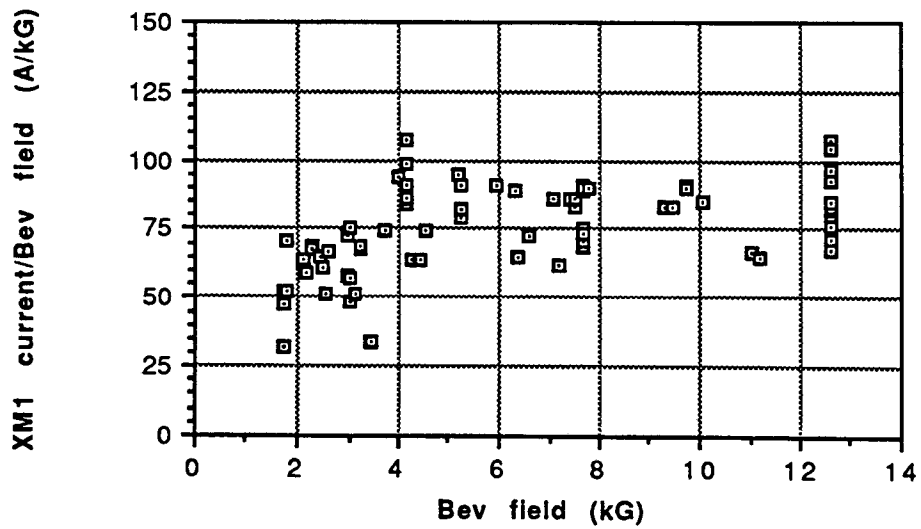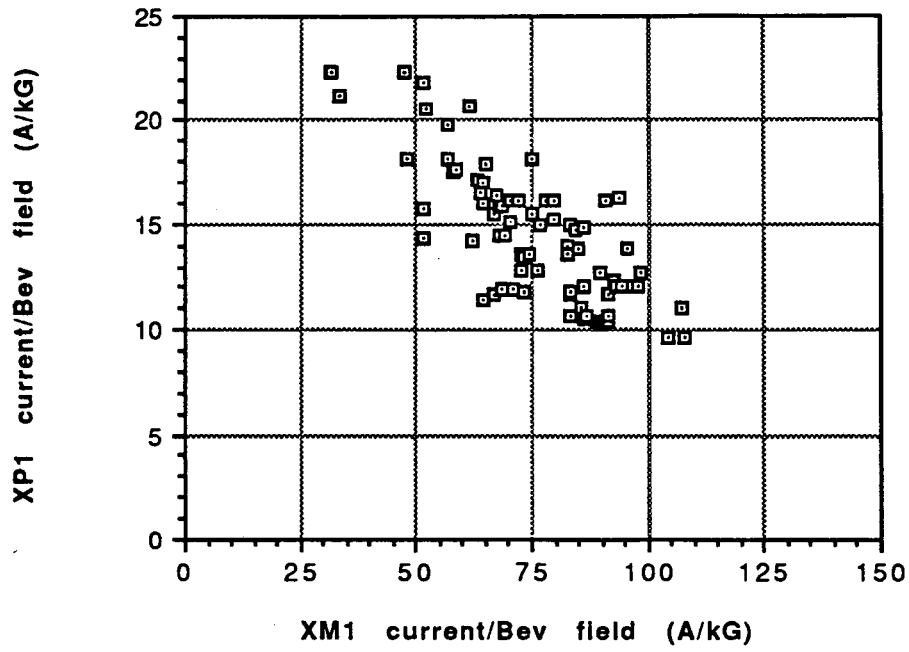
Fig.21
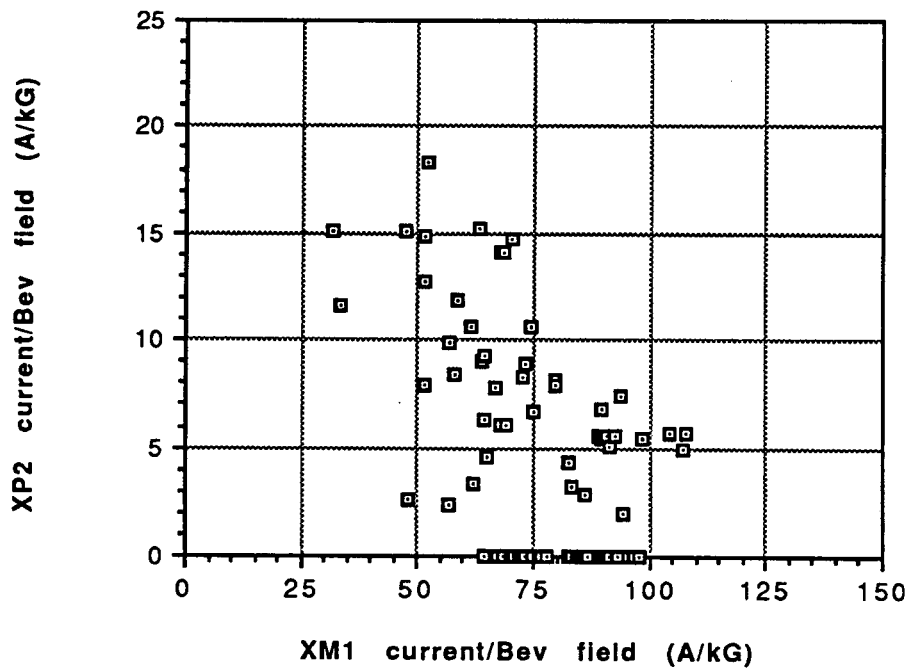
Fig.22
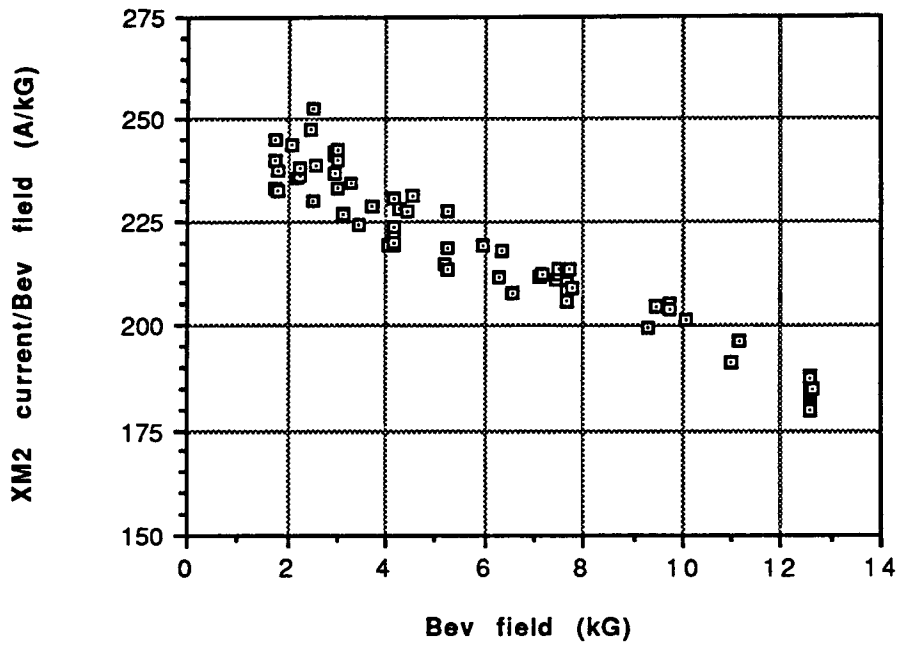
Fig.23
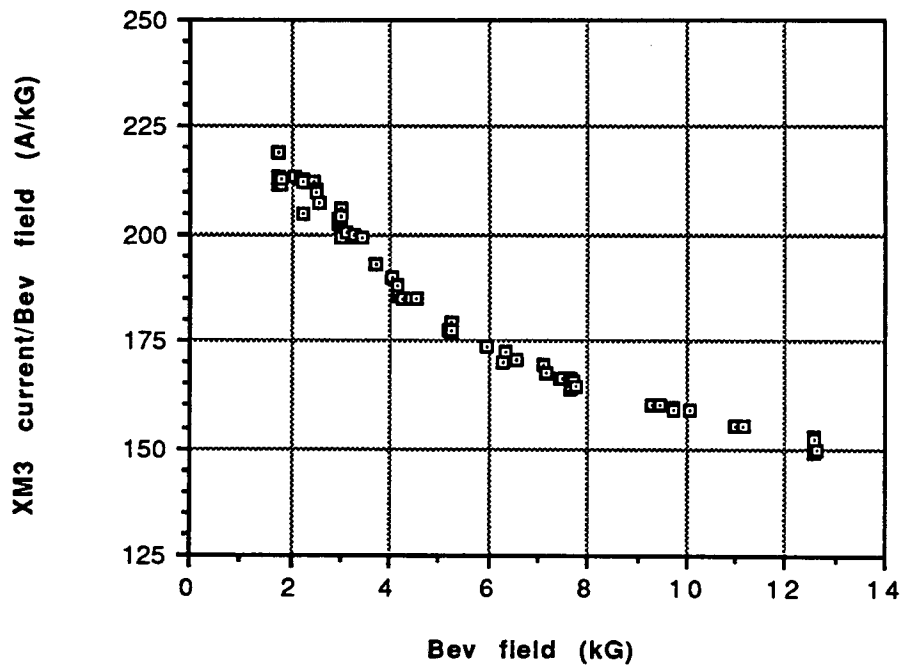
Fig.24
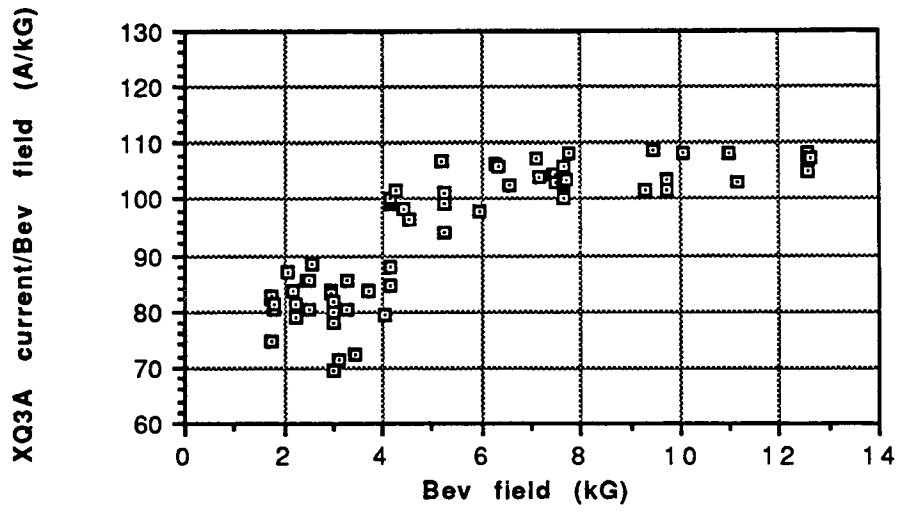
Fig.25(a)
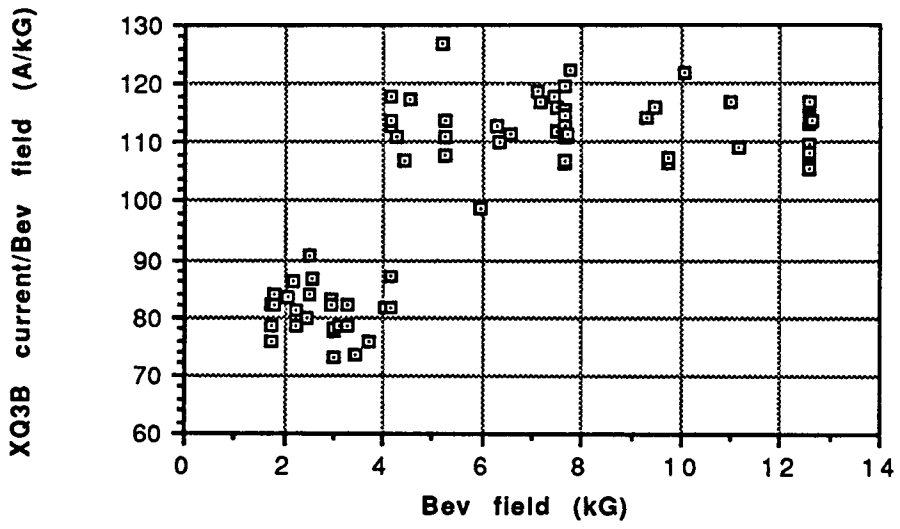
Fig.25(b)
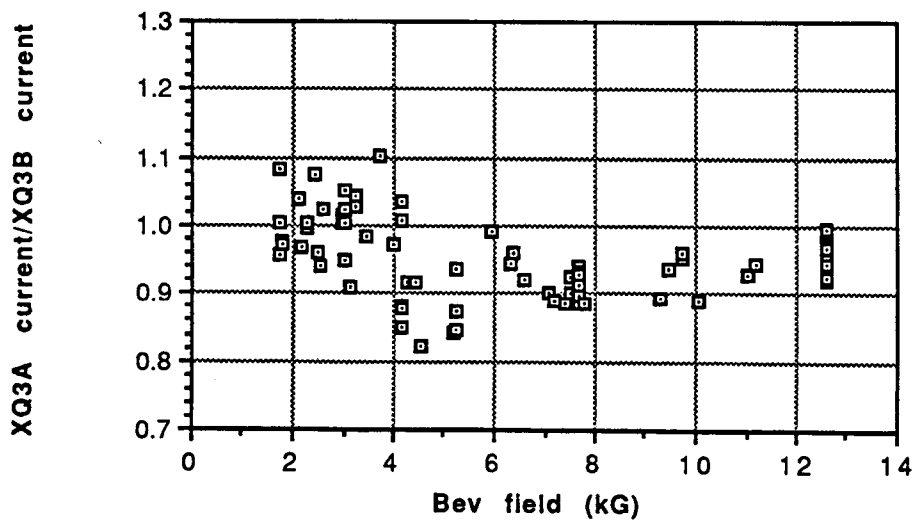
Fig.25(c)
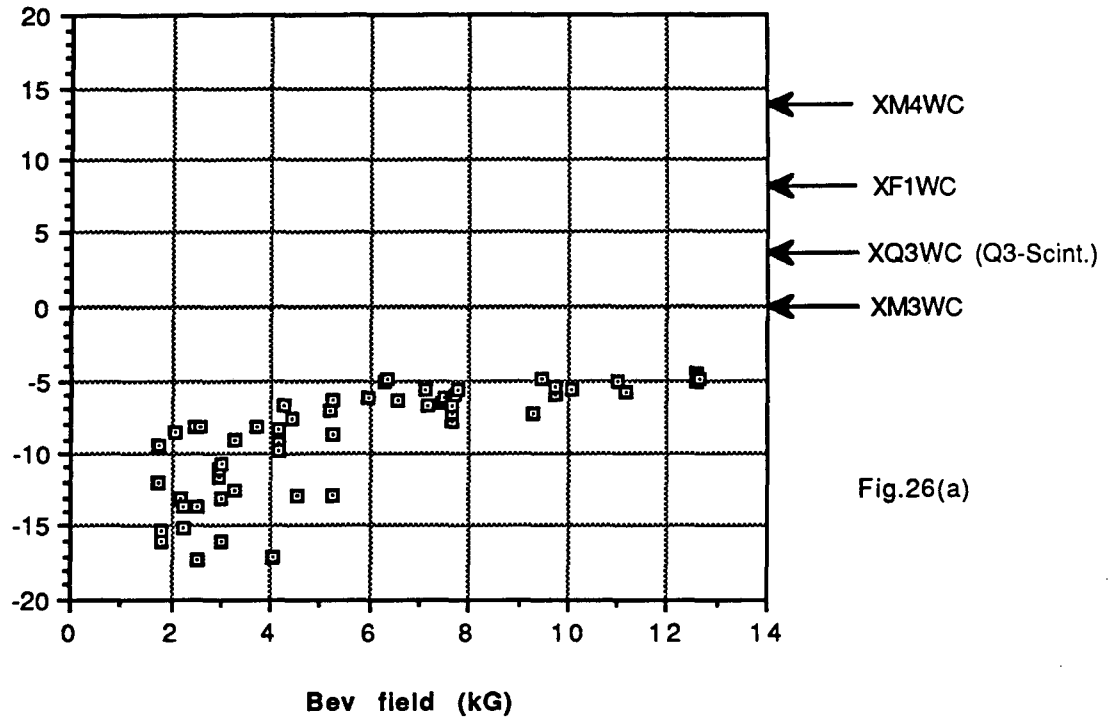
Fig.26(a)

Fig.26(b)
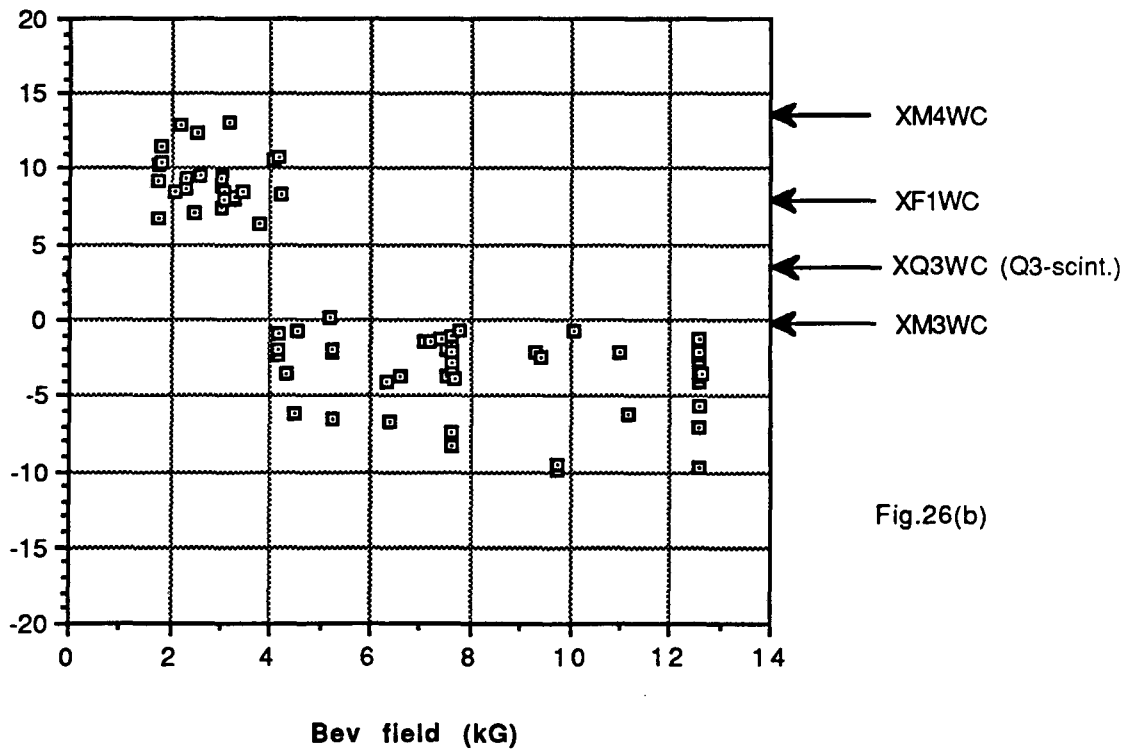
LAWRENCE BERKELEY LABORATORY
UNIVERSITY OF CALIFORNIA
TECHNICAL INFORMATION DEPARTMENT
BERKELEY, CALIFORNIA 94720